

# Glucose-Based Amphiphilic Telomers Designed to Keep Membrane Proteins Soluble in Aqueous Solutions: Synthesis and Physicochemical Characterization

K. Shivaji Sharma,<sup>†</sup> Grégory Durand,<sup>†,\*</sup> Fabrice Giusti,<sup>‡</sup> Blandine Olivier,<sup>†</sup>  
Anne-Sylvie Fabiano,<sup>†</sup> Paola Bazzacco,<sup>‡</sup> Tassadite Dahmane,<sup>‡</sup> Christine Ebel,<sup>#</sup>  
Jean-Luc Popot,<sup>‡</sup> and Bernard Pucci<sup>†,\*</sup>

Laboratoire de Chimie Bioorganique et des Systèmes Moléculaires Vectoriels, Université d'Avignon et des Pays de Vaucluse, Faculté des Sciences, 33 rue Louis Pasteur, F-84000 Avignon, France, Laboratoire de Physico-Chimie Moléculaire des Membranes Biologiques, UMR 7099, CNRS and Université Paris-7, Institut de Biologie Physico-Chimique, 13, rue Pierre-et-Marie-Curie, F-75005 Paris, France, and Laboratoire de Biophysique Moléculaire, CNRS, Institut de Biologie Structurale, (CEA/DSV/IBS, Université Joseph Fourier), 41 rue Jules Horowitz, Grenoble, F-38027, France

Received July 18, 2008. Revised Manuscript Received September 12, 2008

A novel class of nonionic amphipols (NAPols) designed to handle membrane proteins in aqueous solutions has been synthesized, and its solution properties have been examined. These were synthesized through free radical cotelomerization of glucose-based hydrophilic and amphiphilic monomers derived from tris(hydroxymethyl)acrylamidomethane using azobisisobutyronitrile as the initiator and thiol as the transfer agent. The molecular weight and the hydrophilic/lipophilic balance of the cotelomers were modulated by varying the thiol/monomers and the hydrophilic monomer/amphiphilic monomer ratios, respectively, and were characterized by <sup>1</sup>H NMR, UV, gel permeation chromatography, and Fourier transform infrared spectroscopy. Their physicochemical properties in aqueous solution were studied by dynamic light scattering, aqueous size-exclusion chromatography, analytical ultracentrifugation, and surface-tension measurements. NAPols are highly soluble in water and form, within a large concentration range, well-defined supramolecular assemblies with a diameter of ~6–7 nm, a narrow particle size distribution, and an average molecular weight close to 50 × 10<sup>3</sup> g·mol<sup>-1</sup>. Varying the hydrophilic/amphiphilic monomer ratio of NAPols in the range of 3.0–4.9, the degree of polymerization in the range of 51–78, and the resulting average molar mass in the range of 20–29 × 10<sup>3</sup> g·mol<sup>-1</sup> has little incidence on their solution properties. Glucose-based NAPols efficiently kept soluble in aqueous solutions two test membrane proteins: bacteriorhodopsin and the transmembrane domain of *Escherichia coli*'s outer membrane protein A.

## Introduction

Integral membrane proteins (IMPs) represent 20–30% of the proteins encoded in the genomes of cells. Because IMPs are involved in such essential cell functions as bioenergy transduction, transmembrane transfer of nutrients and drugs, cell-to-cell communication, tissue formation, cell adhesion, and so forth, knowledge of their structure, function, and dysfunction is essential to a wide range of biomedical and biotechnological applications. IMPs, however, are difficult to study *in vitro*, largely because of four main factors: low levels of natural abundance, difficult overexpression, insolubility in water, and a limited stability once extracted from biological membranes. The water-insolubility of IMPs is due to the hydrophobic character of that fraction of their surface that, *in situ*, is in contact with the membrane interior. Classically, IMPs are extracted from membranes and handled in aqueous solution using detergents.<sup>1,2</sup> Detergents are dissociating amphiphiles, which dissolve membranes and form water-soluble complexes with both IMPs and lipids. However, they tend to

disrupt the protein/protein, protein/lipid, and protein/cofactor interactions that stabilize the three-dimensional structure of IMPs, leading to inactivation.<sup>1,3,4</sup>

Among many attempts to alleviate this problem is the design and use of milder surfactants such as amphipathic peptides,<sup>5–7</sup> tripod amphiphiles,<sup>8</sup> fluorinated surfactants,<sup>9–12</sup> or specially designed amphipathic polymers called “amphipols” (APols). First introduced by Tribet *et al.*,<sup>13</sup> APols are relatively short single-chain copolymers or terpolymers comprising both polar and apolar side chains, which can substitute to detergents to keep IMPs water-soluble.<sup>14–16</sup> The many alkyl chains carried by APols bind noncovalently to the hydrophobic transmembrane surface of

\* To whom correspondence should be addressed. Phone: +33 4 9014 4445; fax: +33 4 9014 4441; e-mail: gregory.durand@univ-avignon.fr (G.D.). Phone: +33 4 9014 4442; fax: +33 4 9014 4499; e-mail: bernard.pucci@univ-avignon.fr (B.P.).

<sup>†</sup> Université d'Avignon et des Pays de Vaucluse.

<sup>‡</sup> Institut de Biologie Physico-Chimique.

<sup>#</sup> Institut de Biologie Structurale.

(1) Garavito, R. M.; Ferguson-Miller, S. *J. Biol. Chem.* **2001**, *276*, 32403–32406.

(2) le Maire, M.; Champeil, P.; Møller, J. V. *Biochim. Biophys. Acta* **2000**, *1508*, 86–111.

(3) Bowie, J. U. *Curr. Opin. Struct. Biol.* **2001**, *11*, 397–402.

(4) Gohon, Y.; Popot, J.-L. *Curr. Opin. Colloids Interface Sci.* **2003**, *8*, 15–22.

(5) Schafmeister, C. E.; Miercke, L. J.; Stroud, R. M. *Science* **1993**, *262*, 734–738.

(6) McGregor, C.-L.; Chen, L.; Pomroy, N. C.; Hwang, P.; Go, S.; Chakrabarty, A.; Privé, G. G. *Nat. Biotechnol.* **2003**, *21*, 171–176.

(7) Yeh, J. I.; Du, S.; Tortajada, A.; Paulo, J.; Zhang, S. *Biochemistry* **2005**, *44*, 16912–16919.

(8) Yu, S. M.; McQuande, D. T.; Quinn, M. A.; Hackenberger, C. P.; Krebs, M. P.; Polans, A. S.; Gellman, S. H. *Protein Sci.* **2000**, *9*, 2518–2527.

(9) Barthelemy, P.; Ameduri, B.; Chabaud, E.; Popot, J.-L.; Pucci, B. *Org. Lett.* **1999**, *1*, 1689–1692.

(10) Breyton, C.; Chabaud, E.; Chaudier, Y.; Pucci, B.; Popot, J.-L. *FEBS Lett.* **2004**, *564*, 312–318.

(11) Palchevskyy, S. S.; Posokhov, Y. O.; Olivier, B.; Popot, J.-L.; Pucci, B.; Ladokhin, A. S. *Biochemistry* **2006**, *45*, 2629–2635.

(12) Lebaupain, F.; Salvay, A. G.; Olivier, B.; Durand, G.; Fabiano, A.-S.; Michel, N.; Popot, J.-L.; Ebel, C.; Breyton, C.; Pucci, B. *Langmuir* **2006**, *22*, 8881–8890.

(13) Tribet, C.; Audebert, R.; Popot, J.-L. *Proc. Natl. Acad. Sci. U.S.A.* **1996**, *93*, 15047–15050.

IMPs,<sup>17</sup> providing multiple attachment points that render the association quasi-irreversible,<sup>18,19</sup> while the polar groups keep the IMP/APol complex water-soluble. The most widely used APol to date, A8-35, is obtained by derivatization of poly(acrylic acid) with ~25% hydrophobic octylamine and ~40% isopropylamine, leaving ~35% of free carboxylate groups, with an average molar mass of  $9-10 \times 10^3 \text{ g} \cdot \text{mol}^{-1}$ .<sup>13,20</sup> A8-35 self-organizes in aqueous solutions into well-defined particles of  $\sim 40 \times 10^3 \text{ g} \cdot \text{mol}^{-1}$ .<sup>20,21</sup> IMP/A8-35 complexes are well-defined, compact, and stable in solution for extended periods of time (months).<sup>16</sup> As a rule, the biochemical stability of A8-35-trapped IMPs is greatly improved as compared to that in detergent solutions.<sup>13,14,16,22,23</sup> *Escherichia coli* diacylglycerol kinase,<sup>24</sup> *Torpedo marmorata* nicotinic acetylcholine receptor,<sup>25</sup> and *Halobacterium salinarum* bacteriorhodopsin (BR)<sup>16</sup> have all been shown to remain functional as complexes with APols. Sarcoplasmic reticulum  $\text{Ca}^{2+}$ -ATPase, on the other hand, is both stabilized and reversibly inhibited by APols.<sup>22,23</sup> APols can be used to fold IMPs to their active form,<sup>26,27</sup> to immobilize them onto solid supports,<sup>28</sup> and to study them by solution NMR<sup>17</sup> or cryo-electron microscopy.<sup>29</sup>

Other types of APols have been described, including variants of A8-35 with different chain lengths and/or charge densities,<sup>13</sup> a zwitterionic APol,<sup>24,30</sup> sulfonated APols,<sup>23,31</sup> and APols carrying phosphorylcholine polar groups.<sup>32,33</sup> Specific biological applications indeed may require or benefit from particular physicochemical properties. Electroneutrality over an extended pH range, for instance, which none of the above APols provide, is compelling for isoelectrofocusing applications, and desirable for IMP crystallization. This has prompted us to explore the possibility of creating totally nonionic amphipols (NAPols). The feasibility of this approach was first established with a series of NAPols derived from tris(hydroxymethyl)-acrylamidomethane (THAM), which proved able to keep two test IMPs—BR and cytochrome

$b_6 f$ —soluble in the absence of detergent.<sup>34</sup> However, only the two most hydrophobic NAPols of that series led to the formation of low-molecular weight, relatively monodisperse, and stable IMP/NAPol complexes. Because of their high hydrophobicity, these polymers suffered from a relatively low water-solubility ( $< 50 \text{ g} \cdot \text{L}^{-1}$ ), which limited their usefulness in biochemistry.

The present article describes the synthesis and characterization of a novel series of  $\beta$ -D-glucose-based THAM-derived NAPols. NAPols were synthesized by free-radical cotelomerization of THAM-derived hydrophilic and amphiphilic monomers<sup>35</sup> using azobisisobutyronitrile as the initiator and a thiol as the transfer reagent. The hydrophilic/lipophilic balance was tuned by varying the ratio of hydrophilic and amphiphilic monomers. We have examined the self-association properties of the resulting polymers at different concentrations and temperatures using surface tension and dynamic light scattering (DLS) measurements, aqueous size-exclusion chromatography (ASEC), and analytical ultracentrifugation (AUC). We show that glucose-based NAPols present an excellent water solubility and a high surface activity, and that they self-organize, in a concentration-independent manner, into compact, small particles with a well-defined size. Such properties have previously been shown to condition the formation of well-defined IMP/APol complexes suitable for biophysical and biochemical research.<sup>16</sup> Glucose-based NAPols indeed kept soluble in aqueous solutions two test membrane proteins with very different folds: BR and the transmembrane domain of *E. coli*'s outer membrane protein A.

## Experimental Section

Materials, general procedures and instrumentation for the synthesis, and synthesis of compounds **1** and **2** are given in the Supporting Information.

**Synthesis of Cotelomer.** Monomers **A** and **B** (or **B'**) at the chosen A/B ratio (a total concentration of 3.0 mM) were dissolved in tetrahydrofuran (THF). The mixture was heated at reflux under argon. According to Mayo's equation<sup>36</sup> ( $1/\text{DP}_n = \text{Ct} \times [\text{telogen}]/[\text{monomers}]$ ) and considering that the transfer constant Ct of TA is close to 1, an appropriate volume of TA (0.03 mM) and AIBN (0.5 equiv) dissolved in THF was added through a syringe, and the reaction mixture was stirred at reflux under argon until complete consumption of the monomers ( $\sim 12-24$  h). The mixture was concentrated under vacuum and purified by Sephadex LH-20, eluting with MeOH/CH<sub>2</sub>Cl<sub>2</sub> (1:1 v/v), to give the cotelomer as a white powder ( $\sim 75\%$ ).

**Deprotection.** The transformation of protected cotelomers into water-soluble NAPols was achieved under mild basic conditions. Acetylated cotelomers (200 mg) were dissolved in methanol (20 mL) under argon, and a catalytic amount of sodium methoxide was added. After 12 h of being stirred at ambient temperature,  $\sim 1.0$  g of IRC-50 resin was added to neutralize the solution. The mixture was shaken for 15 min followed by filtration and concentrated under vacuum. The resulting oil was dissolved in methanol (2.0 mL) and precipitated in cold ether (50 mL). After filtration, the polymer was dried under vacuum to give NAPol (90%) as a white powder.

**Dialysis.** An aqueous solution of NAPol ( $10 \text{ mg} \cdot \text{mL}^{-1}$ ) was passed through a  $0.45 \mu\text{m}$  filter and dialyzed against water under continuous stirring. The exterior water was monitored through UV and changed every 4 h until no absorbance was observed. The resulting dialyzed solution was freeze-dried from water, then lyophilized to give pure NAPol ( $\sim 60\%$ ) as a white foam.

**Polymer Analyses.** a. *Monomers Ratio (x/y) by <sup>1</sup>H NMR.* The monomer ratio (x/y) in the protected cotelomer was estimated by comparing the well-defined peak integrals assigned to three specific protons from glucose moieties (H<sub>4</sub>, H<sub>3</sub>, and H<sub>2</sub>) between  $\delta = 4.8-5.3$

(14) Popot, J.-L.; Berry, E. A.; Charvolin, D.; Creuzenet, C.; Ebel, C.; Engelmann, D. M.; Flötenmeyer, M.; Giusti, F.; Gohon, Y.; Hervé, P.; Hong, Q.; Lakey, J. H.; Leonard, K.; Shuman, H. A.; Timmins, P.; Warschawski, D. E.; Zito, F.; Zoonens, M.; Pucci, B.; Tribet, C. *Cell. Mol. Life Sci.* **2003**, *60*, 1559–1574.

(15) Sanders, C. S.; Hoffmann, A. K.; Gray, D. N.; Keyes, M. H.; Ellis, C. D. *ChemBioChem* **2004**, *5*, 423–426.

(16) Gohon, Y.; Dahmane, T.; Ruigrok, R.; Schuck, P.; Charvolin, D.; Rappaport, F.; Timmins, P.; Engelmann, D. M.; Tribet, C.; Popot, J.-L.; Ebel, C. *Biophys. J.* **2008**, *94*, 3523–3537.

(17) Zoonens, M.; Catoire, L. J.; Giusti, F.; Popot, J.-L. *Proc. Natl. Acad. Sci. U.S.A.* **2005**, *102*, 8893–8898.

(18) Tribet, C.; Audebert, R.; Popot, J.-L. *Langmuir* **1997**, *13*, 5570–5576.

(19) Zoonens, M.; Giusti, F.; Zito, F.; Popot, J.-L. *Biochemistry* **2007**, *46*, 10392–10404.

(20) Gohon, Y.; Giusti, F.; Prata, C.; Charvolin, D.; Timmins, P.; Ebel, C.; Tribet, C.; Popot, J.-L. *Langmuir* **2006**, *22*, 1281–1290.

(21) Gohon, Y.; Pavlov, G.; Timmins, P.; Tribet, C.; Popot, J.-L.; Ebel, C. *Anal. Biochem.* **2004**, *334*, 318–334.

(22) Champeil, P.; Menguy, T.; Tribet, C.; Popot, J.-L.; le Maire, M. *J. Biol. Chem.* **2000**, *275*, 18623–18637.

(23) Picard, M.; Dahmane, T.; Garrigos, M.; Gauron, C.; Giusti, F.; le Maire, M.; Popot, J.-L.; Champeil, P. *Biochemistry* **2006**, *45*, 1861–1869.

(24) Gorzelle, B. M.; Hoffman, A. K.; Keyes, M. H.; Gray, D. N.; Ray, D. G.; Sanders, C. R. *J. Am. Chem. Soc.* **2002**, *124*, 11594–11595.

(25) Martinez, K. L.; Gohon, Y.; Corringier, P.-J.; Tribet, C.; Mérola, F.; Changeux, J.-P.; Popot, J.-L. *FEBS Lett.* **2002**, *528*, 251–256.

(26) Pocanschi, C. L.; Dahmane, T.; Gohon, Y.; Rappaport, F.; Apell, H.-J.; Kleinschmidt, J. H.; Popot, J.-L. *Biochemistry* **2006**, *45*, 13954–13961.

(27) Dahmane, T.; Damian, M.; Popot, J.-L.; Banères, J.-L. Submitted to *Biochemistry*, 2008.

(28) Charvolin, D.; Perez, J.-B.; Rouvière, F.; Giusti, F.; Abdine, A.; Martinez, K. L.; Popot, J.-L. Submitted to *Proc. Natl. Acad. Sci. U.S.A.*, 2008.

(29) Flötenmeyer, M.; Weiss, H.; Tribet, C.; Popot, J.-L.; Leonard, K. *J. Microsc.* **2007**, *227*, 229–235.

(30) Nagy, J. K.; Hoffmann, A. K.; Keyes, M. H.; Gray, D. N.; Oxenoid, K.; Sanders, C. R. *FEBS Lett.* **2001**, *501*, 115–120.

(31) Dahmane, T.; Giusti, F.; Catoire, L. J.; Popot, J.-L. In preparation.

(32) Diab, C.; Winnik, F. M.; Tribet, C. *Langmuir* **2007**, *23*, 3025–3035.

(33) Diab, C.; Tribet, C.; Gohon, Y.; Popot, J.-L.; Winnik, F. M. *Biochim. Biophys. Acta* **2007**, *1768*, 2737–2747.

(34) Prata, C.; Giusti, F.; Gohon, Y.; Pucci, B.; Popot, J.-L.; Tribet, C. *Biopolymers* **2001**, *56*, 77–84.

(35) Sharma, K. S.; Durand, G.; Pucci, B., In preparation, 2008.

(36) Mayo, F. R.; Lewis, F. M. *J. Am. Chem. Soc.* **1944**, *66*, 1594–1601.

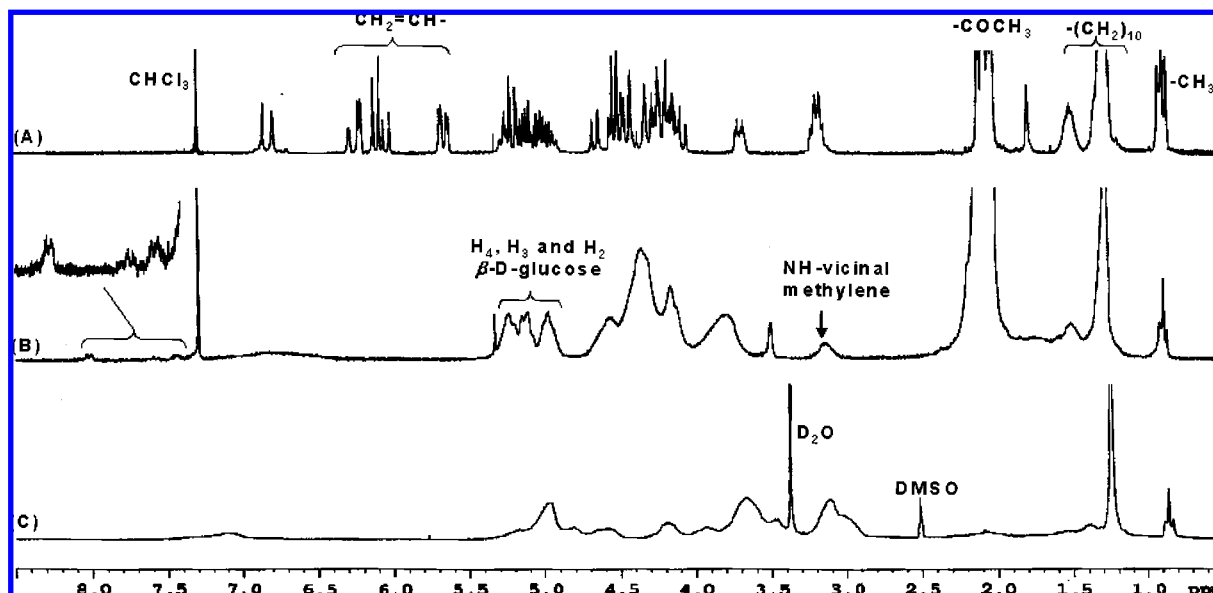


**Figure 1.**  $^1\text{H}$  NMR spectra of (A) monomer **B'** (in  $\text{CDCl}_3$ ), (B) acetylated NA20-78 (in  $\text{CDCl}_3$ ), and (C) deprotected NA20-78 (in  $\text{DMSO}-d_6$ ).

ppm from both the monomers **A** and **B** (or **B'**) with the NH-vicinal methylene group of the alkyl chain at  $\delta = 3.15$  ppm from only monomer **B** (or **B'**) in  $^1\text{H}$  NMR spectra (Figure 1B). The number average degree of polymerization (DP<sub>n</sub>) of cotelomer was determined by combining  $^1\text{H}$  NMR and UV data (see Supporting Information for further details).

*b. Determination of  $M_n$  by UV-Vis Spectroscopy.* The  $M_n$  value of the protected cotelomers, which leads to  $x$  and  $y$  values, was measured by a UV absorbance method. The three benzoyl groups grafted on the tris(hydroxymethyl)aminomethane (Tris) moiety of the transfer agent lead to a strong absorbance in UV at  $\lambda = 272$  nm (molar absorptivity coefficient,  $\epsilon = 2.8 \times 10^3 \text{ L} \cdot \text{mol}^{-1} \cdot \text{cm}^{-1}$ ). In a first step, a calibration curve of the telogen absorbance versus its molar concentration is established by using standard solution at 10–580  $\mu\text{M}$  in  $\text{CH}_2\text{Cl}_2/\text{MeOH}$  (1:1 v/v) (see Figure S3). Subsequently, three different samples of cotelomer were analyzed: in each case, a precise weight of cotelomer was dissolved in  $\text{CH}_2\text{Cl}_2/\text{MeOH}$ , defining the weight concentration of polymer in  $\text{g} \cdot \text{L}^{-1}$ , and this solution was diluted at a concentration suitable for UV measurements. The value of absorbance measured in UV provided the molar concentration of the transfer agent [TA(M)] in the solution. The average molecular mass of the cotelomer,  $M_n$  was then calculated by the following equation, with errors within  $\pm 3\%$ :

$$M_n = [\text{cotelomer}(\text{g} \cdot \text{L}^{-1})]/[\text{TA}(\text{M})] \quad (1)$$

*c. Gel Permeation Chromatography (GPC).* GPC measurements were made on a Waters system equipped with a differential refractive index detector on two sets of column systems at 45 °C: (1) Styragel HR 4, 3, and 2 (4.6  $\times$  300 mm),  $\bar{M}_w = 5 \times 10^2$  to  $5 \times 10^5 \text{ g} \cdot \text{mol}^{-1}$ , using eluent THF or THF + 0.01% trifluoroacetic acid (TFA) at a flow rate of 0.3  $\text{mL} \cdot \text{min}^{-1}$ , and (2) Styragel HT 5 and 3 (7.8  $\times$  300 mm),  $\bar{M}_w = 5 \times 10^2$  to  $4 \times 10^6 \text{ g} \cdot \text{mol}^{-1}$ , using eluent dimethylformamide (DMF) or DMF + 0.01 M LiBr at a flow rate of 1  $\text{mL} \cdot \text{min}^{-1}$ . Polymethylmethacrylate (PMMA;  $\bar{M}_p = 7.8 \times 10^3$  to  $1.85 \times 10^5 \text{ g} \cdot \text{mol}^{-1}$ ) from Polymer Laboratories, Ltd., U.K., was used for calibration. In both systems, the sample concentration was 5  $\text{mg} \cdot \text{mL}^{-1}$ , and injection volume was 10  $\mu\text{L}$  without filtration. Data were analyzed using Waters Millennium Empower 2.0 software.

**Dynamic Light Scattering.** NAPols at different concentrations and temperatures were determined by a Zetasizer Nano-S model 1600 (Malvern Instruments, Ltd., U.K.) equipped with a He-Ne laser ( $\lambda = 633$  nm, 4.0 mW). The average decay rate was obtained from the measured autocorrelation function using the method of cumulants employing a quadratic fit. The time-dependent correlation function of the scattered light intensity was measured at a scattering

angle of 173° relative to the laser source. The hydrodynamic diameter ( $D_H$ ) of the particles was estimated from their diffusion coefficient using the Stokes–Einstein equation. The variation from one measurement to the next was  $\sim 5\%$ .

**Aqueous Size-Exclusion Chromatography.** NAPol (100 mg) was dissolved in Milli-Q water (1 mL). This stock solution (100  $\mu\text{L}$ ) was diluted in Tris buffer (900  $\mu\text{L}$ ). A 100  $\mu\text{L}$  of the latter mixture were injected on a Superose 12 10-300GL column (bed volume: 20 mL; void volume: 7.5 mL; separation range:  $D_H = 2$ –18 nm) connected to a purifier 10 Äkta system (GE-Healthcare) and calibrated according to the procedure reported elsewhere.<sup>20,21</sup>

**Density and Analytical Sedimentation Velocity (SV) Experiments.** NA20-78 powder was placed at 4 °C and protected from light under vacuum in a desiccator over phosphorus pentoxide for 7 weeks in order to reduce the residual water content in the samples. Two samples of 9.810 and 5.132  $\text{g} \cdot \text{L}^{-1}$  were prepared by precisely weighing (at  $10^{-5}$  g accuracy) NAPol and water. We used a DMA 5000 (Anton PAAR) to measure at 20 °C the difference in density,  $\Delta\rho$  ( $\text{g} \cdot \text{mL}^{-1}$ ), between these samples and the reference solvent water of density  $\rho^\circ$ , as a function of NAPol concentration,  $c$  (here, in  $\text{g} \cdot \text{mL}^{-1}$ ). From  $\Delta\rho/c = 1 - \rho^\circ \bar{v}$ , we determine  $\bar{v} = 0.724 \pm 0.006 \text{ mL} \cdot \text{g}^{-1}$  for NA20-78. These samples and dilutions at 2.44 and 0.95  $\text{g} \cdot \text{L}^{-1}$  were used for SV experiments conducted in an XLI analytical ultracentrifuge (Beckman, Palo Alto, CA) using an ANTi-50 rotor, at 42 000 rpm and 20 °C for 11 h. Data acquisition was made at 280 nm and using interference optics. For each sample, a set of SV profiles was treated globally using the analysis in terms of a continuous distribution of sedimentation coefficients,  $c(s)$ , of the program Sedfit<sup>37</sup> (freely available at: <http://www.analyticalultracentrifugation.com>). Sedfit also incorporates a systematic noise evaluation procedure. Integration of the peak under the  $c(s)$  peaks gives estimates of the sedimentation coefficients of the different species and of their concentration, in signal units (absorbance or number of fringes). The linear fit  $s/s_0 = (1 - k_s c)$  provides an estimate of the sedimentation coefficient at infinite dilution,  $s_0$ , and of the concentration dependency factor,  $k_s$ . The values of  $s_0$  were interpreted through the Svedberg equation:

$$s_0 = M(1 - \rho^\circ \bar{v})/N_A 3\pi\eta^\circ D_H \quad (2)$$

where  $M$  is the molecular mass, and  $N_A$  is Avogadro's number.

**Surface Tension Measurement.** The surface activity of NAPols in solution at an air–water interface was determined by the Wilhelms plate technique using a Krüss K-100 tensiometer (Krüss, Germany) at  $20 \pm 0.5$  °C. The polymer solution (20 mL) was poured into a

(37) Schuck, P *Biophys. J.* **2000**, *78*, 1606–1619.

thermostatted glass trough, and the surface tension was determined at increasing dilutions. For each measurement, the standard deviation was found not to exceed  $0.02 \text{ mN}\cdot\text{m}^{-1}$ . Other conditions were as reported elsewhere.<sup>12,38</sup>

**Nonionic Amphipol/Membrane Protein Complexes: Preparation and Solubility in Aqueous Solutions.** *Bacteriorhodopsin.* Purple membrane was purified<sup>39</sup> from *H. salinarum*, strain S9 (a gift from G. Zaccari, ILL, Grenoble, France). A sample suspended at  $6 \text{ g}\cdot\text{L}^{-1}$  in 20 mM sodium phosphate buffer, pH 7.0, was solubilized by incubation for 40 h at 4 °C in the dark with 100 mM octylthioglucoside (OTG; critical micellar concentration (cmc)  $\approx 9 \text{ mM}$ ). After centrifugation for 20 min at  $200\,000 \times g$  in the TLA 100.2 rotor of a TL 100 ultracentrifuge (Beckman Coulter, France), the supernatant was diluted to 18 mM OTG with detergent-free buffer. Aliquots of NAPol stock solutions ( $10 \text{ g}\cdot\text{L}^{-1}$  in water) were added to 50- $\mu\text{L}$  samples to reach final protein/polymer mass ratios of 1:5–1:10. The samples were incubated for 20 min at 4 °C, diluted 3-fold with surfactant-free buffer (100 mM NaCl, 20 mM sodium phosphate buffer, pH 7.0; final OTG concentration: 6 mM), incubated for 1 h at 4 °C, and centrifuged for 20 min at  $200\,000 \times g$ . The concentration of BR in the solution before and after centrifugation was estimated using  $\epsilon_{554} = 47 \text{ mM}^{-1}\cdot\text{cm}^{-1}$  and  $\epsilon_{280} = 81 \text{ mM}^{-1}\cdot\text{cm}^{-1}$ .<sup>40</sup> As a control, solubility was assayed with BR trapped with APol A8-35, BR in 18 mM OTG, and BR in 6 mM OTG.

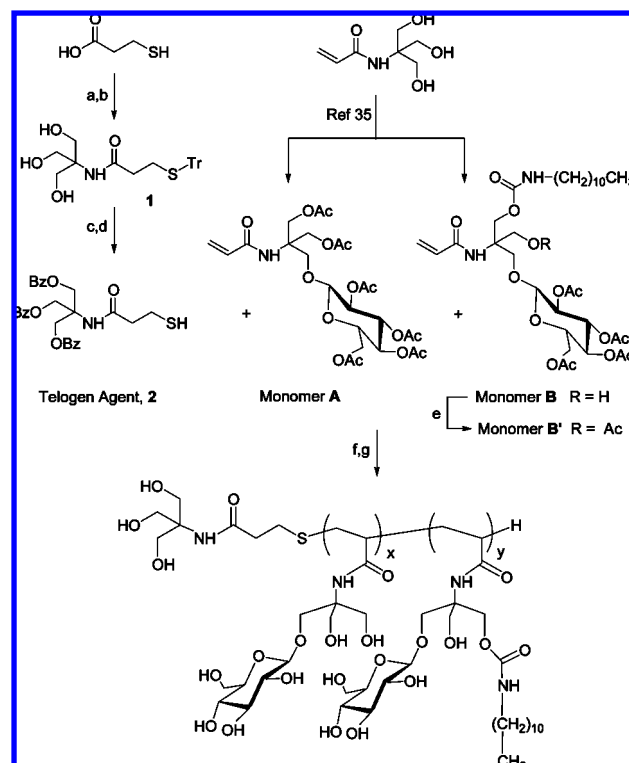
*tOmpA.* A stock solution of the purified 171-residue transmembrane domain of outer membrane protein A from *E. coli* (tOmpA; a gift from G.E. Schulz, Freiburg University, Freiburg-im-Breisgau, FRG) was prepared as described previously.<sup>17</sup> The final solution contained 60  $\mu\text{M}$  tOmpA in 20 mM tetraethylene glycol monoethyl ether ( $\text{C}_8\text{E}_4$ ; cmc  $\approx 7 \text{ mM}$ ) in 20 mM Tris/HCl buffer, 100 mM NaCl, pH 8.0. The concentration of tOmpA was determined from the absorbance at 280 nm using  $\epsilon_{280} = 46\,470 \text{ M}^{-1}\cdot\text{cm}^{-1}$ , established by amino acid analysis.<sup>17</sup> Aliquots of NAPol stock solutions ( $10 \text{ g}\cdot\text{L}^{-1}$  in water) were added to 10- $\mu\text{L}$  samples to reach final protein/polymer mass ratios of 1:2–1:20, incubated for 20 min at 4 °C, adjusted to 200  $\mu\text{L}$  with surfactant-free buffer (final  $\text{C}_8\text{E}_4$  concentration: 1 mM), incubated for 30 min at 4 °C, and centrifuged for 20 min at  $200\,000 \times g$ . The concentration of tOmpA in the solution before and after centrifugation was determined spectroscopically. As a control, solubility was assayed with tOmpA trapped with APol A8-35, tOmpA in 20 mM  $\text{C}_8\text{E}_4$ , and tOmpA in 1 mM  $\text{C}_8\text{E}_4$ .

## Results and Discussion

**Synthesis of Amphiphilic Cotelomers.** The synthesis of NAPols is based on three key steps (Scheme 1): (i) synthesis of the thiol-based transfer agent, (ii) synthesis of acetylated hydrophilic **A** and amphiphilic **B** or **B'** monomers derived from THAM,<sup>35</sup> and (iii) free-radical cotelomerization.

The telogen agent (TA) **2** was synthesized in four consecutive steps from 3-mercaptopropionic acid. The thiol group was first protected by reaction with triphenylmethylchloride in dichloromethane, then Tris was grafted through an amide bond onto the protected 3-mercaptopropionic acid in the presence of 2-ethoxy-1-ethoxycarbonyl-1,2-dihydroquinoline (EEDQ) in refluxing ethanol. The three hydroxyl functions of the resulting compound **1** were protected by benzoyl groups by reaction with an excess of benzoyl chloride in the presence of triethylamine (TEA). Lastly, removal of the protective group of the thiol by TFA in dichloromethane (2:8 v/v) led, after purification, to TA **2** with 41% yield from 3-mercaptopropionic acid. Triethylsilane ( $\text{Et}_3\text{SiH}$ ) was used as scavenger of the triphenylmethyl cation formed during the cleavage of the thioether bond, so as to reduce the side reactions of this highly reactive intermediate. The synthesis of monomers **A**, **B**, and **B'** will be published as

Scheme 1. Synthetic pathway of NAPols<sup>a</sup>



<sup>a</sup> Reagents and conditions: (a)  $\text{Ph}_3\text{CCl}$  (1.1 equiv),  $\text{CH}_2\text{Cl}_2$ , rt, 16 h, 95%; (b) Tris (1.1 equiv), EEDQ (1.2 equiv.), EtOH, 50 °C, 12 h, 79%; (c)  $\text{PhCOCl}$  (4.5 equiv), TEA (9 equiv.),  $\text{CH}_2\text{Cl}_2$ , rt, 12 h, 92%; (d) TFA/ $\text{CH}_2\text{Cl}_2$  (2:8 v/v),  $\text{Et}_3\text{SiH}$ , 0 °C, 4 h, 60%; (e)  $\text{Ac}_2\text{O}/\text{Pyr}$  (1:1 v/v), rt, 12 h, 97%; (f) AIBN (0.5 equiv), THF, Ar, 66 °C, 8–24 h, 75%; (g) MeONa, MeOH, pH 8–9, rt, 12 h, 90%.

described.<sup>35</sup> Before proceeding to cotelomerization, the TA was fully characterized by  $^1\text{H}$ ,  $^{13}\text{C}$ , DEPT NMR sequences and mass spectrometry (see Figures S1 and S2 in the Supporting Information).

Radical cotelomerization was carried out in refluxing THF in the presence of compound **2** (1.0 equiv) as the transfer reagent and AIBN (0.5 equiv) as the initiator. The relative composition of monomers ( $x/y$ ) in the protected cotelomers were determined by the respective initial ratio of acetylated hydrophilic monomer **A** to acetylated amphiphilic monomer **B** or **B'**, while the number average degree of polymerization ( $\text{DP}_n$ ) was correlated to the initial ratio of both monomers to TA **2** ( $R_0$ ) considering the transfer constant of TA ( $\text{Ct}$ ) close to 1, as described for various alkyl thiol transfer reagents.<sup>41</sup> The polymerization reaction was monitored by thin layer chromatography (TLC; ethyl acetate/cyclohexane, 7:3 v/v) as the spots of TA ( $R_f \approx 0.8$ ), monomer **A** ( $R_f \approx 0.4$ ), and monomers **B/B'** ( $R_f \approx 0.4$  and  $R_f \approx 0.6$ , respectively) disappear and a new spot with  $R_f \approx 0$  emerges. Because the  $R_f$  of monomer **A** and monomer **B** are very close, the accurate monitoring of the reaction was sometimes uncertain. This is the reason why monomer **B'** was finally preferred, since its spot does not overlap with that of monomer **A**. The resulting acetylated cotelomers were purified by SEC on a Sephadex LH-20 column, which removed the low molecular weight compounds, such as remaining monomers and short telomers like dimers, trimers, and so forth. The purified polymers were found to be readily soluble in common organic solvents such as methanol, chloroform, dichloromethane, THF, or toluene, as well as in

(38) Ortial, S.; Durand, G.; Poeggeler, B.; Polidori, A.; Pappolla, M. A.; Boker, J.; Hardeland, R.; Pucci, B. *J. Med. Chem.* **2006**, *49*, 2812–2820.

(39) Oesterhelt, D.; Stoekenius, W. *Methods Enzymol.* **1974**, *31*, 667–678.

(40) London, E.; Khorana, H. G. *J. Biol. Chem.* **1982**, *257*, 7003–7011.

(41) Starks, C. M. *Free Radical Telomerizations*; Academic Press: New York, 1974.

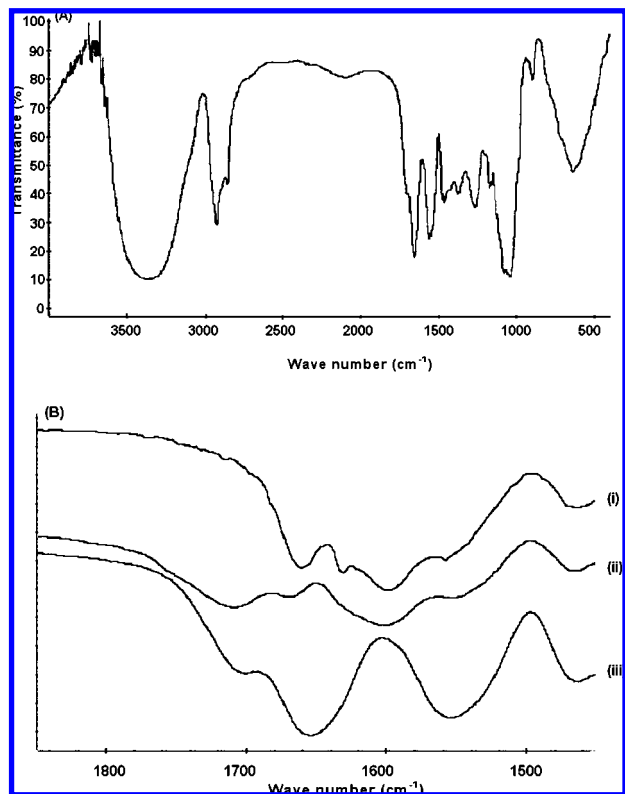


**Figure 2.** Fourier transform infrared (FTIR) spectra of (A) deprotected NA25-78, from wavenumber 400  $\text{cm}^{-1}$  to 4000  $\text{cm}^{-1}$  and (B) (i) deprotected monomer **A**, (ii) deprotected monomer **B**, and (iii) NA25-78, from wavenumber 1400  $\text{cm}^{-1}$  to 1800  $\text{cm}^{-1}$ .

polar aprotic solvents such as DMF. Deacetylation was achieved by Zemlén's reaction, followed by precipitation in methanol/ether. The deprotected polymers were dialyzed against water using cellulose membranes and lyophilized, yielding pure NAPols.

Figure 1 shows the  $^1\text{H}$ NMR spectra of monomer **B'**, acetylated cotelomer NA20-78, and deprotected NA20-78. It can be seen that the  $^1\text{H}$ NMR signal at  $\delta = 5.6\text{--}6.3$  ppm of the acryloyl protons in monomer **B'** (Figure 1A) disappeared during cotelomerization (Figure 1B), whereas the other signals broadened. The disappearance of the acetyl ( $-\text{COCH}_3$ ) proton signal at  $\delta = 2.0\text{--}2.3$  ppm and the absence of a hump from the three phenyl groups at  $\delta = 7.4\text{--}8.1$  ppm in the cotelomer (Figure 1C) testify of the completion of the deprotection reaction.

Representative IR spectra of deprotected monomers **A** and **B** and of a NAPol are given in Figure 2. The characteristic broadband between 3100 and 3700  $\text{cm}^{-1}$  originates from the hydrophilic part of the polymer (i.e., the hydroxyl groups), while peaks around 1700–1650  $\text{cm}^{-1}$  are attributed to carbonyl groups (Figure 2A). The characteristic peak located at  $\sim 1665$   $\text{cm}^{-1}$  is due to the conjugated carbonyl group of the amide bond from monomers **A** and **B** or **B'**, while the peak at  $\sim 1700$   $\text{cm}^{-1}$  denotes the carbonyl group of the urethane bond, which is only present in monomer **B** or **B'** (Figure 2B). This last peak was also observed in the final NAPols. The peak due to the carbonyl group of the amide bond, on the other hand, shifted slightly to a lower wavenumber (1654  $\text{cm}^{-1}$ ), as a result of the absence of conjugation in the final polymer.<sup>42</sup> Monomers also show a peak at 1600  $\text{cm}^{-1}$ , which corresponds to strong double-bond stretching vibrations; this peak disappears in NAPols as a result of polymerization.

**Polymer Characterization.** The ratio,  $x/y$ , between monomers **A** and **B** in the protected cotelomers was determined by  $^1\text{H}$ NMR (see Experimental Section and Supporting Information for further details). As expected, the resolution of the spectra was fairly poor, although significantly higher for the acetylated compounds in  $\text{CDCl}_3$  than for the deprotected ones in dimethyl- $d_6$ -sulfoxide ( $\text{DMSO-}d_6$ ; Figure 1B,C). Generally, the DPn of short telomers can be determined by  $^1\text{H}$ NMR, by comparing the integral of a signal assigned to the TA to that of at least one peak due to the monomers.<sup>43</sup> However, when the size of the telomer increases, this technique becomes inaccurate. We thus introduced onto the TA a benzoyl group, which exhibits a strong UV absorption ( $\lambda_{\text{max}} = 272$  nm) and can be easily removed in basic media. A calibration curve for the UV absorbance of the TA was first established (see Figure S3 in Supporting Information). The UV spectrum of a solution of telomer of known mass concentration was then recorded, which yielded the molar concentration of TA in the solution. Since each cotelomer backbone contains a single TA, the average molecular mass of the cotelomer can be derived [at the same concentration used for the UV calibration ( $\sim 10$   $\text{g}\cdot\text{L}^{-1}$ ), no absorbance was observed at  $\lambda = 272$  nm for a cotelomer devoid of phenyl groups]. As followed by  $^1\text{H}$ NMR, no degradation of the benzoyl group was observed when the pure TA was reacted with AIBN in refluxing THF. This demonstrates that, during the course of the telomerization reaction, the ester bond of the TA is stable. Combining this information and the  $x/y$  ratio from  $^1\text{H}$ NMR (see below) allows one to determine the DPn of the NAPols, even when the molecular mass is high. For the sake of comparison, we also determined the molecular weight of the cotelomer by comparing, in the acetylated and benzoylated cotelomer, the  $^1\text{H}$ NMR integral area of the peaks due to protons from the three phenyl groups of the TA ( $\delta = 7.4\text{--}8.1$  ppm) with those originating from the typical glucose protons ( $\text{H}_4$ ,  $\text{H}_3$ ,  $\text{H}_2$ ,  $\delta = 4.8\text{--}5.3$  ppm), which are common to monomers **A**, **B**, and **B'** (Figure 1B). The molecular weight obtained by  $^1\text{H}$ NMR was found to be in good agreement with that obtained by UV. However, due to the extent of errors in the NMR technique, molecular weights determined by UV absorbance are more accurate in the present context.

Weight average molecular weight and number average molecular weight ( $\bar{M}_w$  and  $\bar{M}_n$ ) as well as polydispersity ( $\bar{M}_w/\bar{M}_n$ ) of the protected cotelomers were also determined by GPC, using PMMA as a standard. A number of different solvents were used: THF, THF + 0.1% TFA, DMF, and DMF + 0.1 M LiBr. Results obtained in THF and DMF + 0.1 M LiBr are reported in Table 1. Other results are presented in the Supporting Information (Table S1), as well as GPC analyses of different cotelomers (Figure S4).

When THF was used as solvent, protected cotelomers eluted very late, as though they had a very low average molecular weight, namely  $3.5\text{--}7.1 \times 10^3$   $\text{g}\cdot\text{mol}^{-1}$ , as compared to that ( $30\text{--}50 \times 10^3$   $\text{g}\cdot\text{mol}^{-1}$ ) determined by UV measurements. These results may indicate either a possible adsorption of the cotelomers on the column or a much smaller hydrodynamic volume than expected, possibly due to intramolecular associations, a combination of both effects being of course possible. The latter effect could arise from the relatively high polarity of these cotelomers (even if they are still protected) and the use of a weakly polar solvent. This could lead to a collapse of the polymeric backbone, resulting in a decrease of the hydrodynamic volume. There are precedents for such an effect. For instance, inconsistencies have been reported in molecular weight determinations by GPC of

(42) Rao, C. N. R. *Chemical Applications of Infrared Spectroscopy*; Academic Press: New York and London, 1963.

(43) Contino, C.; Maurizis, J. C.; Ollier, M.; Rapp, M.; Lacombe, J. M.; Pucci, B. *Eur. J. Med. Chem.* **1998**, *33*, 809–816.

**Table 1. Average Molecular Weight (g·mol<sup>-1</sup>) of Different Protected Cotelomers by UV, NMR, and GPC**

NAPol (protected)	UV <sup>a</sup> $\bar{M}_n/10^3$	NMR <sup>b</sup> $\bar{M}_n/10^3$	GPC <sup>c</sup>					
			THF			DMF + 0.01 M LiBr		
			$\bar{M}_w/10^3$	$\bar{M}_n/10^3$	PDI	$\bar{M}_w/10^3$	$\bar{M}_n/10^3$	PDI
NA22-75	36	38.3	4.7	3.8	1.26	12.6	11.9	1.06
NA25-78	40	41.8	4.8	3.1	1.35	13.5	12.6	1.07
NA22-83	36	42.0	3.4	3.1	1.13	11.9	11.5	1.04
NA29-83	48	48.1	7.1	4.4	1.61	14.4	13.5	1.07
NA20-78 <sup>d</sup>	31	35.3	5.0	4.0	1.26	13.4	12.7	1.06

<sup>a</sup> Determined from UV absorbance of the TA in CH<sub>2</sub>Cl<sub>2</sub>/MeOH (1:1, v/v). <sup>b</sup> Estimated by integrating the <sup>1</sup>H NMR peaks of three protons of glucose ( $\delta = 4.8$ –5.3 ppm) and those from the phenyl group of the TA ( $\delta = 7.3$ –8.1 ppm) in CDCl<sub>3</sub>. <sup>c</sup> Weight-average molecular weight, number-average molecular weight, and polydispersity Index ( $\bar{M}_w/\bar{M}_n$ ) were evaluated using PMMA calibrant. <sup>d</sup> Synthesized with monomer B'. The nomenclature for cotelomers is explicated in the legend to Table 2.

**Table 2. Synthesis Conditions and Structural Composition of Different NAPols**

NAPol <sup>a</sup>	molar ratio of monomers		$R_0^c$	DPn		average $\bar{M}_n/10^3 \pm 1 \times 10^3(\text{g}\cdot\text{mol}^{-1})$		mean number of monomers per molecule	
	$x_0/y_0$	$x/y$ (actual) <sup>b</sup>		UV <sup>d</sup>	NMR <sup>e</sup>	protected <sup>f</sup>	deprotected	$x$	$y$
NA22-75	3:1	3:1	60	57 ± 3	62 ± 3	36	22	~43 (~75%)	~14 (~25%)
NA25-78	4:1	3.5:1	100	64 ± 3	68 ± 3	40	25	~50 (~78%)	~14 (~22%)
NA22-83	5:1	5:1	90	59 ± 3	69 ± 4	36	22	~49 (~83%)	~10 (~17%)
NA29-83	6:1	4.9:1	100	78 ± 4	79 ± 4	48	29	~65 (~83%)	~13 (~17%)
NA20-79	4:1	3.6:1	60	52 ± 3	50 ± 3	33	20	~41 (~79%)	~11 (~21%)
NA20-78 <sup>e</sup>	4:1	3.5:1	50	51 ± 3	58 ± 3	31	20	~40 (~78%)	~11 (~22%)

<sup>a</sup> In amphipol short names, "NA" stands for "nonionic amphipol" and is followed by two numbers referring to the average molecular weight of the deprotected polymer as determined by UV (in kg·mol<sup>-1</sup>) and to the percentage of hydrophilic monomer A, respectively. <sup>b</sup> Determined by <sup>1</sup>H NMR (CDCl<sub>3</sub>) of protected cotelomers. <sup>c</sup> Initial molar ratio of monomer (A+B) to TA. <sup>d</sup> Estimated by combining UV and <sup>1</sup>H NMR analyses. <sup>e</sup> Estimated by comparing the signals from three protons of glucose with that of the phenyl group of the TA in <sup>1</sup>H NMR. <sup>f</sup> Determined from UV absorbance of the TA. <sup>g</sup> Synthesized with monomer B'.

poly-*N*-isopropylacrylamide as compared to other methods.<sup>44</sup> It was concluded that the discrepancies observed between GPC and chain end determination at low molecular weight may arise from the nonideal variation of the hydrodynamic volume with molecular weight. In the case of protected NAPols, the irreliability of GPC measurements seems obvious. TFA, frequently used as a buffer in liquid chromatography for separation of organic compounds, was added (at 0.1% v/v) to THF in order to investigate the possible effect of the solvent on interactions with the column. This resulted in an apparent increase of  $\bar{M}_w$  and  $\bar{M}_n$  by ~20% (except for NA29-83), which is far from explaining the discrepancy with the value determined by UV titration (Table 1). Substituting DMF for THF resulted in a 2–3-fold increase in apparent  $\bar{M}_w$  and  $\bar{M}_n$ , thus demonstrating that changing the polarity of the solvent significantly affects the retention time. Polar solvents may affect either the hydrodynamic volume of the polymeric chain or the interactions of the macromolecules with the polystyrene-based column. As reported by several authors,<sup>45–48</sup> supplementing DMF with LiBr resulted in a slight increase of  $\bar{M}_w$  and  $\bar{M}_n$  as compared to pure DMF, with  $\bar{M}_w$  values in the range of ~12–15 × 10<sup>3</sup> g·mol<sup>-1</sup>. This, nevertheless, remains inferior by a factor of ~3 to estimates obtained by UV measurements. Similar unreliable GPC measurements have been reported for polygermane<sup>49</sup> and organosilane polymers.<sup>50</sup> At variance with the latter measurements, however, the distribution of NAPols upon GPC was essentially unimodal, the shape of the peaks being symmetrical, with no evidence of oligomeric or

unreacted species (Figure S4) (as is also demonstrated by the absence of signals from the acryloyl group of monomers in <sup>1</sup>H NMR; see Figure 1B). As a further note of caution, one should note that GPC values are calibrated with PMMA and, therefore, have to be taken as merely indicative, since such a calibration may lead to questionable results when the polarity and backbone stiffness of the cotelomers studied deviate strongly from those of the standards.

As a final cause for caution, we note that the exceptionally low polydispersity of NAPols upon GPC (~1.06 and ~1.32 in DMF + 0.01 M LiBr and in THF, respectively) is quite unusual for polymers obtained by conventional radical polymerization,<sup>51</sup> an observation that may cast additional suspicion on the GPC results.

Further attempts were also carried out using a wide variety of commonly used solvent systems, such as THF + 0.1% tetra-*n*-butylammonium bromide,<sup>52,53</sup> THF + 2 g·L<sup>-1</sup> LiNO<sub>3</sub>,<sup>54</sup> and DMF + 0.02 M KNO<sub>3</sub>. In THF mixed solvent systems,  $\bar{M}_w$  values ranged from ~5 to 6 × 10<sup>3</sup> g·mol<sup>-1</sup>, while, in DMF mixed systems, they were closer to ~11–12 × 10<sup>3</sup> g·mol<sup>-1</sup>. Considering the inconsistencies in  $\bar{M}_w$  and  $\bar{M}_n$  determination obtained by GPC, the UV technique was deemed much more accurate, and the values thus obtained were used for further physicochemical and biological assays. Optimizing GPC conditions for the analysis of NAPols is under progress, but is beyond the scope of the present article.

Table 2 summarizes the composition data of different batches of cotelomers. NAPols are denoted by a short name reflecting their structural parameters: the letters NA stand for "nonionic amphipol", followed by the average molecular weight (in g·mol<sup>-1</sup> × 10<sup>-3</sup>) determined by UV analysis of the deprotected NAPols,

(44) Ganachaud, F.; Monteiro, M. J.; Gilbert, R. G.; Dourges, M.-A.; Thang, S. H.; Rizzardo, E. *Macromolecules* **2000**, *33*, 6738–6745, and references therein.

(45) Mei, Y.; Beers, K. L.; Byrd, H. C. M.; VanderHart, D. L.; Washburn, N. R. *J. Am. Chem. Soc.* **2004**, *126*, 3472–3476.

(46) Deming, T. J. *J. Am. Chem. Soc.* **1997**, *119*, 2759–2760.

(47) Yamamoto, T.; Abe, M.; Wu, B.; Choi, B. K.; Harada, Y.; Takahashi, Y.; Kawata, K.; Sasaki, S.; Kubota, K. *Macromolecules* **2007**, *40*, 5504–5512.

(48) Moon, D. K.; Osakada, K.; Maruyama, T.; Kubota, K.; Yamamoto, T. *Macromolecules* **1993**, *26*, 6992–6997.

(49) Katz, S. M.; Reichl, J. A.; Berry, D. H. *J. Am. Chem. Soc.* **1998**, *120*, 9844–9849.

(50) Cotts, P. M.; Miller, R. D.; Trefonas, P. T.; West, R.; Fickes, G. N. *Macromolecules* **1987**, *20*, 1046–1052.

(51) Isaure, F.; Cormack, P. A. G.; Sherrington, D. C. *React. Funct. Polym.* **2006**, *66*, 65–79.

(52) Carriedo, G. A.; Soto, A. P.; Valenzuela, M. L.; Tarazona, M. P.; Saiz, E. *Macromolecules* **2008**, *41*, 1881–1885.

(53) Karatas, Y.; Pyckhout-Hintzen, W.; Zorn, R.; Richter, D.; Wiemhofer, H.-D. *Macromolecules* **2008**, *41*, 2212–2218.

(54) Siebourg, W.; Lundberg, R. D.; Lenz, R. W. *Macromolecules* **1980**, *13*, 1013–1016.

**Table 3. Particle Size Distribution Parameters of Different NAPols Derived from ASEC and DLS in Aqueous Solution at 25°C**

NAPol	ASEC			$D_H^d$ from DLS (HHW) <sup>e</sup>				
	$V_e^a$ (mL)	$D_H^b$ ( $\pm 0.4$ nm)	HHW <sup>c</sup> (mL)	concentration ( $\text{g}\cdot\text{L}^{-1}$ )				
				100	80	50	25	10
NA22-75	13.0	5.8	0.8	7.2 (1.8)	6.9 (1.8)	6.6 (1.6)	6.7 (1.7)	6.5 (1.8)
NA25-78	13.1	5.4	0.8	6.8 (1.9)	6.5 (1.9)	6.4 (1.9)	6.2 (1.9)	6.1 (1.8)
NA22-83	12.6	6.6	0.7	6.3 (2.0)	6.2 (1.8)	6.1 (1.8)	5.8 (1.8)	5.6 (1.8)
NA29-83	12.9	5.8	0.9	6.8 (2.8)	6.8 (2.7)	6.2 (3.6)	6.2 (4.1)	6.0 (2.1)
NA20-79	12.7	6.4	1.0	6.6 (1.6)	<sup>f</sup>	<sup>f</sup>	<sup>f</sup>	6.2 (1.6)
NA20-78	13.2	5.8	0.7	6.4 (2.0)	6.4 (1.8)	6.3 (1.8)	6.1 (1.7)	6.1 (1.8)
A8-35	12.5 <sup>g</sup>	6.4	0.9	<sup>f</sup>	<sup>f</sup>	<sup>f</sup>	<sup>f</sup>	<sup>f</sup>

<sup>a</sup> Elution volume of the main peak of particles. <sup>b</sup> Hydrodynamic diameter as determined from calibration with soluble proteins (see ref 20). <sup>c</sup> HHW, the width of the peak at half-height, an indication of the degree of polydispersity of the aggregates. <sup>d</sup> Hydrodynamic diameter of particles of the main peak. <sup>e</sup> Width of the peak at half-height. <sup>f</sup> Not determined in this series of measurements. <sup>g</sup> Measurements carried out in parallel for the polyacrylate-based APol A8–35<sup>20</sup> are given for comparison.

followed by the percentage of monomer **A**. For instance, “NA25-78” denotes an NAPol with  $M_w \approx 25 \times 10^3 \text{ g}\cdot\text{mol}^{-1}$ , comprising 78% of monomer **A**. In Table 2, the columns  $x_0/y_0$  and  $R_0$  indicate the initial molar ratios of monomers **A/B** and **(A+B)/TA**, respectively. Various NAPols were obtained by varying the ratio of monomers and TA in the reaction batch, with  $3 < (x_0/y_0) < 6$  and  $50 < R_0 < 100$  (see rows 1–4 in Table 2). The monomer ratio  $(x/y)_{\text{actual}}$  was kept between 3 and 5, corresponding to 75–83% (molar ratio) of monomer **A** and 17–25% of monomer **B**. A series of NAPols with constant  $(x_0/y_0) = 4$  and different  $R_0$  values was also synthesized. The NAPols of this series have a constant monomer ratio, with  $(x/y)_{\text{actual}} = 3.5 \pm 0.1$ , i.e., 78% hydrophilic monomer **A** and 22% amphiphilic monomer **B**, whereas their average molecular mass varied. As shown in Table 2, the initial  $R_0 = [\text{Monomers}/\text{TA}]$  used in the reaction batches roughly sets the DPn of the resulting cotelomers (the experimental DPn measured by <sup>1</sup>H NMR and, more precisely, by UV determination are close to one another). In most batches, the final DPn was found to be lower than the initial  $R_0$  value, suggesting that the telomer transfer constant might be slightly higher than 1. However, we observed that the difference between  $R_0$  and DPn increases with  $R_0$  for  $R_0 < 50$ –60. This may be due to a collapse of the polymeric chain (as already suggested by the GPC data) during the course of telomerization in THF, leading to an inhibition of the growth of the macroradical.

#### Physicochemical Properties of NAPols in Aqueous Solutions.

For biological applications, it is essential that APols be highly soluble in water ( $>50 \text{ g}\cdot\text{L}^{-1}$ ). Figure S5 illustrates the determination of the aqueous solubility of NA25-78 (i.e., a NAPol with an average molecular mass of  $25 \times 10^3 \text{ g}\cdot\text{mol}^{-1}$  and 78% hydrophilic monomer **A**). All NAPols were found to be highly soluble in water ( $>100 \text{ g}\cdot\text{L}^{-1}$ ), except for NA22-75. The relatively poor solubility of NA22-75 ( $<90 \text{ g}\cdot\text{L}^{-1}$ ) reflects its more pronounced hydrophobic character, due to a higher proportion (25%) of partially hydrophobic residues. Aqueous solutions of NAPols were transparent and remained fluid up to a concentration of  $100 \text{ g}\cdot\text{L}^{-1}$ , above which they became gradually oily viscous.

**Dynamic Light Scattering.** NAPol stock solutions at  $100 \text{ g}\cdot\text{L}^{-1}$  in water were stored overnight before DLS measurements. All of them were found to form well-defined particles, 6–7 nm in diameter, above  $\sim 0.06 \text{ g}\cdot\text{L}^{-1}$ , with an average polydispersity of  $<1.9$  nm. (Table 3). No interpretable signal was measured at lower concentrations. The particles exhibit a remarkable consistency in size and size distribution, whatever the polymer molecular weight and the ratio of hydrophilic to hydrophobic monomers. Nevertheless, the particle diameter formed by the most hydrophobic polymer, NA22-75, appears to be  $\sim 5\%$  higher than that found for the other NAPols, while that of the least

hydrophobic polymer, NA22-83, appears to be  $\sim 5\%$  lower. Figure S6 shows the evolution as a function of concentration of the hydrodynamic diameter of the particles formed, in water at 25 °C, by different NAPols. Upon increasing the concentration up to  $100 \text{ g}\cdot\text{L}^{-1}$ , the size of the particles does not drastically change, but it increases slightly (by  $\sim 10\%$ ) yet significantly in a monotonous manner. The particle distribution was stable for weeks at 25 °C. Indeed, the particle size of 1-month-old solutions was found to be similar to that of fresh solutions, and no large aggregate formation was observed during prolonged storage. There is no phase separation as well as no significant change in the dimension of the aggregates between 1 and  $100 \text{ g}\cdot\text{L}^{-1}$  and temperatures between 10 and 80 °C (see Tables S2 and S3). Figure S7 shows the hydrodynamic diameter distribution of different NAPols under different conditions.

**Aqueous Size-Exclusion Chromatography.** ASEC provides an alternative approach to analyzing the size and homogeneity of particles resulting from amphiphilic polymer intermolecular associations in aqueous media.<sup>20,21</sup> Before the dialysis step, ASEC revealed a heterogeneous size distribution: a small amount of very large particles eluted in the void volume ( $V_0$ ) at 7.5 mL, a main peak between 12.5 and 13 mL ( $D_H = 6$ –8 nm), and smaller particles (or contaminants) beyond 15 mL ( $D_H < 4$  nm) (Figure S8). Dialysis efficiently removes small impurities eluting between 15 and 24 mL, most probably low molecular weight polymers (Figure S8). NMR analysis of the impurities yielded a weakly resolved spectrum, quite similar to that of NAPols, suggesting a polymeric nature. However, the water solubility was found to be extremely low ( $<25 \text{ g}\cdot\text{L}^{-1}$ ) when compared to that of NAPols, indicative of a more hydrophobic character. As shown in Figure 3, the ASEC profile of dialyzed NAPols is very similar to that of A8-35, an APol known to form well-defined particles ( $D_H = 6.3$  nm).<sup>20</sup>

The small apparent diameter and narrow size distribution of the particles is generally consistent with that determined by DLS (Table 3). Indeed, a fair consistency between the particles size of A8-35 determined by DLS and by SEC was already reported,<sup>20</sup> the values by DLS being slightly higher.

**Analytical Ultracentrifugation Sedimentation Velocity Experiments.** SV experiments were performed on NA25-78 samples at 1, 2.5, 5.1, and  $9.8 \text{ g}\cdot\text{L}^{-1}$ . Figure 4 presents the data and fit for the sample at  $2.5 \text{ g}\cdot\text{L}^{-1}$ , and the superimposition of the  $c(s)$  curves for the four concentrations. A main species at  $s \approx 4$  S (80% of the interference signal) is found in addition to smaller species at  $s \approx 1$  S (15%) and larger aggregates between  $s \approx 7$  and 20 S (5%). The  $s$  value of the major species is consistent (see below) with the hydrodynamic diameter distribution observed by DLS. However, in the latter case, the minor species were not resolved. The ratio of the various species does not vary significantly

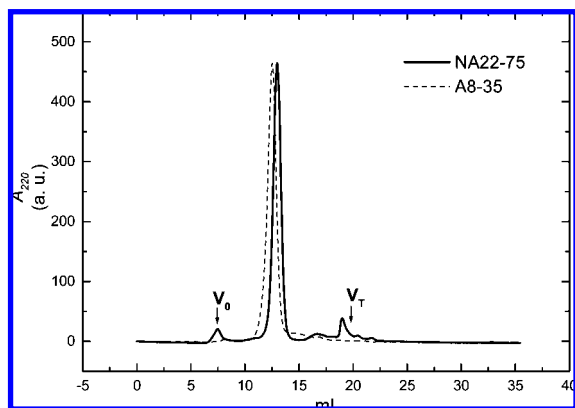


**Figure 3.** ASEC of NAPols NA22-75 and A8-35 on a Superose 12 10-300 GL column (Tris-HCl 20 mM, NaCl 100 mM, pH = 8.5) at 20 °C. The two polymers were detected by their absorbance at 220 nm, and the chromatograms were normalized to the same maximum.

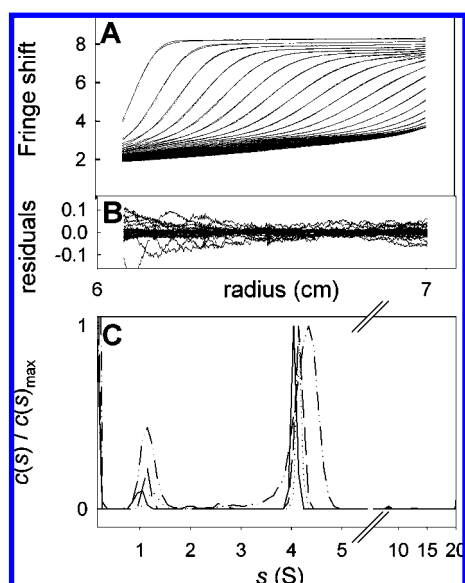


**Figure 4.** SV analysis of NA20-78. (A) Superimposition of selected experimental and modeled SV profiles obtained over 11 h at 42 000 rpm and 20 °C, using interference optics, for water-solubilized NA20-78 at 2.5 g·L<sup>-1</sup>. (B) Corresponding residuals. (C) Superimposition of the  $c(s)$  distributions obtained for NA20-78 at 9.81 (solid line), 5.13 (long dash), 2.44 (dotted) and 0.95 (dash-dot-dot) g·L<sup>-1</sup>. For clarity, the  $c(s)$  scale is normalized to a maximum value of 1.

with sample concentration. The  $s$  value for the main species appears to decrease slightly upon increasing the concentration. From the values of the sedimentation coefficient at infinite dilution,  $s_0 = 4.22 \pm 0.02$  S, and of  $D_H$  from light scattering ( $D_H = 6.1$  nm), a value of  $M \approx 53 \times 10^3$  g·mol<sup>-1</sup> for the molar mass of the particles can be derived using Svedberg's equation. The frictional ratio  $ff_{\min}$  is the ratio of the hydrodynamic diameter to the minimum diameter from the volume ( $\bar{v}M/N_A$ ) of the anhydrous polymer. For a globular, compact particle, the value of  $ff_{\min}$  is usually in the range 1.15–1.3.<sup>55</sup> Using the partial specific volume  $\bar{v} = 0.724$  mL·g<sup>-1</sup> estimated from density measurements (see Experimental Section), we calculate for NA25-78 an  $ff_{\min}$  value of 1.24. Using the value  $D_H = 5.2$  nm from ASEC yields comparable estimates, with  $M \approx 45 \times 10^3$  g·mol<sup>-1</sup> and  $ff_{\min} \approx 1.11$ . NAPols thus form globular and compact particles in aqueous solutions.

(55) Cantor, C. R.; Schimmel, P. R. In *Biophysical Chemistry: Techniques for the Study of Biological Structure and Function. Part II*; Freeman: San Francisco, 1980; pp 344–846.

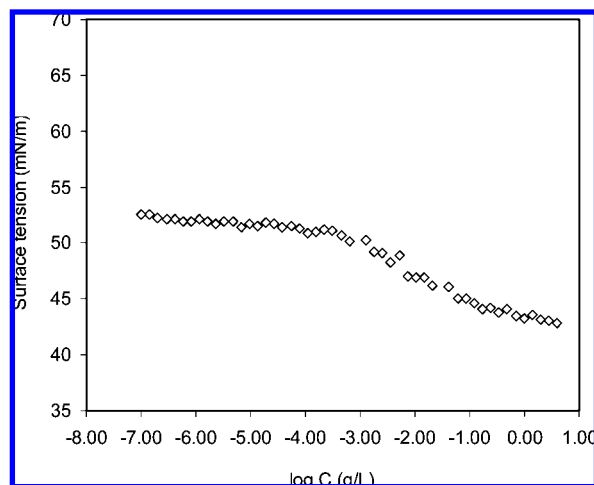


**Figure 5.** Evolution of the surface tension of aqueous solutions of NA20-78 as a function of concentration at 20 °C.

Can the concentration dependency of  $s$  and  $D$  be due to weak interparticle interactions? From the DLS data presented above, we estimate (see Experimental Section) the concentration dependency factors of the sedimentation and diffusion coefficients,  $k_s = 4 \pm 2$  mL·g<sup>-1</sup> and  $k_D = -0.55 \pm 0.15$  mL·g<sup>-1</sup>, respectively. The value of  $k_s$  is related to hydrodynamic nonideality, while  $k_D$  also depends on thermodynamic nonideality.<sup>56,57</sup> The virial term  $2 A_2M$  ( $A_2$  in mL·mol·g<sup>-2</sup>) can be derived from  $k_s$  and  $k_D$ , since  $k_D \approx 2 A_2M - k_s$ .

From this relation, we derive an experimental estimate for  $2 A_2M$  of  $+3.5 \pm 2$  mL·g<sup>-1</sup>. This positive value indicates a regime of globally repulsive interactions, in qualitative agreement with the large solubility of NAPols. However, the quantitative estimate of  $2 A_2M$  is below the minimum value of  $8 \bar{v} = 5.8$  mL·g<sup>-1</sup> expected for noninteracting hard spheres.<sup>58</sup> For the latter, a positive value of  $k_D = +0.2 \times 2 A_2M \approx +0.7$  mL·g<sup>-1</sup> would be expected, while our experimental estimate for  $k_D$  is slightly but significantly negative. Thus, both the low value of  $2 A_2M$  and the negative value of  $k_D$  suggest the existence of a weak attractive contribution to the mean interparticle interactions, while the positive character of  $A_2$  indicates globally repulsive interactions. This apparent paradox probably originates from a slight and monotonous increase in NAPol particle size and mass with concentration, in keeping with DLS data.

**Surface Activity of NAPols at the Air/Water Interface.** Detergents are amphiphilic compounds which form micelles above a critical concentration called the cmc. Micelles are dynamic structures typically of a few nanometers in diameter and a molecular weight of less than 100 kDa. A constant and fast exchange occurs between micellar detergent and free detergent molecules in solution. It is typical for detergents to reduce the surface tension of water to 20–35 mN·m<sup>-1</sup> when their concentration exceed the cmc. Figure 5 shows the evolution as a function of concentration of the surface tension of aqueous solutions of NA20-78 at 20 °C. NAPols are amphiphilic in nature, and indeed they are highly surface-active.

At variance with detergent solutions, whose surface tension ceases to drop once the cmc is reached and the chemical potential

(56) Pusey, P. N.; Tough, R. J. A. In *Dynamic Light Scattering: Applications of Photon Correlation Spectroscopy, Particle Interactions*; Plenum Press: New York, 1985; pp 85–179.

(57) Solovyova, A.; Schuck, P.; Costenaro, L.; Ebel, C. *Biophys. J.* **2001**, *81*, 1868–1880.

(58) Tanford, C. *Physical Chemistry of Macromolecules*; Wiley: New York, 1961.

**Table 4. Ability of NAPols to Keep IMPs Soluble in Aqueous Solutions<sup>a</sup>**

rows	APols	batch	MP/APol w/w ratio	tOmpA in supernatant	native BR in supernatant
1	none		1:0 ([detergent] > CMC)	97%	98%
2	none		1:0 ([detergent] < CMC)	7%	6%
3	A8-35	FRH5	1:4–1:5	98%	100%
4	NA22-75	SS084	1:2	34%	— <sup>b</sup>
5			1:10	— <sup>b</sup>	84%
6	NA25-78	SS078	1:5–1:10	— <sup>b</sup>	82–83%
7	NA22-83	SS061	1:4–1:5	64%	58%
8			1:10–1:20	80%	81%
9	NA29-83	SS081	1:5	— <sup>b</sup>	71%
10			1:10	— <sup>b</sup>	81%
11	NA20-79	SS127	1:2	39%	— <sup>b</sup>
12			1:4–1:5	75%	73%
13			1:10–1:20	73%	89%

<sup>a</sup> Detergent solutions of two test proteins, tOmpA and BR, were supplemented with NAPols at the final protein/polymer mass ratio indicated, incubated for 20 min, diluted under the cmc of the detergent, incubated for 30 min (tOmpA) or 1 h (BR), and centrifuged for 20 min at  $200\,000 \times g$  (see Experimental Section). The fraction of protein present in the supernatant was estimated from its absorbance at 280 nm (tOmpA, BR) and 554 nm (BR). Controls included dilution in the absence of polymer with a solution of detergent above its cmc (row 1) or with buffer (row 2), and dilution with buffer in the presence of the anionic APol A8-35 (row 3). The native-like  $A_{280}/A_{554}$  ratio observed after transferring BR to glucosylated NAPols is an indication of their ability to preserve the protein's native three-dimensional structure. <sup>b</sup> Not determined.

of the monomer stabilizes, the surface tension–concentration plot of NAPol shows a continuous small decrease (by  $\sim 10$  mN/m) from  $10^{-6}$  g/L to 4 g/L. The surface tension drops to  $\sim 40$  mN/m for [NA20-78] =  $\sim 4$  g/L. Marchant and colleagues observed similar features for amphiphilic nonionic poly(vinylamine)-derived oligosaccharide polymers decorated with hydrophobic hexanoyl or fluorocarbon chains.<sup>59,60</sup>

**Ability of Glucose-Based NAPols to Keep Membrane Proteins Soluble in Aqueous Solutions.** APols were designed to keep IMPs soluble in aqueous media. To test the ability of glucose-based NAPols to carry out this function, we chose two IMPs with very different folds: BR, an  $\alpha$ -helical archbacterial plasma membrane protein, and tOmpA, the transmembrane domain of *E. coli*'s outer membrane protein A, an eight-strand  $\beta$ -barrel. OmpA is comprised of two domains, one of them transmembrane and the other periplasmic; tOmpA is the notation for the construct comprising only the transmembrane domain. Using a classical protocol,<sup>13</sup> detergent solutions of each IMP were supplemented (or not) with various NAPols in various protein/polymer mass ratios, and the samples were diluted with buffer under the cmc of the detergent, incubated, and centrifuged. In the absence of polymers, this procedure results in the precipitation of nearly all of the protein (Table 4, row 2). In the presence of detergent above its cmc (row 1) or of APol A8-35 at protein/APol mass ratios of either 1:4 or 1:5 (row 3), all of the protein remained soluble. Intermediate results were obtained with NAPols at 1:2 mass ratio (rows 4 and 11), as is also the case at this ratio of A8-35 (not shown). Except for NA22-83, which may have been slightly less efficient (row 7), the fraction of soluble IMP rose to  $\sim 80\%$  for IMP/NAPol ratios between 1:4–1:20 w/w (rows 5, 6, 8, 10, 12, 13). The slightly lower ratio as compared to that observed with A8-35 ( $\sim 100\%$ ) is likely due to the higher density of NAPols, which must result in denser mixed particles, which sediment faster. The physicochemical properties of IMP/NAPol complexes will be characterized in detail elsewhere. tOmpA is an extremely rugged protein, whose structure is not likely to be affected by transferring it to NAPols. BR, on the other hand, is easily denatured once solubilized. The presence of an absorbance peak at  $\sim 554$  nm in solution reflects the presence of its cofactor, retinal, bound to its intact binding site (the peak of retinal shifts to 380 nm upon BR denaturation).<sup>39</sup>

## Conclusion

In this article, we have described the synthesis and properties of a novel family of nonionic  $\beta$ -D-glucose-based amphiphilic cotelomers with an adjustable hydrophilic/hydrophobic balance. These novel NAPols were obtained by radical telomerization, in the presence of a TA, of two monomers having respectively hydrophilic and amphiphilic properties. Two different techniques were applied to determining the molecular weight of the resulting telomers, namely, GPC and the titration of an end group by either UV or <sup>1</sup>H NMR spectroscopy. GPC, however, was observed to strongly underestimate the molecular weight of protected NAPols, particularly when weakly polar solvents are used. This suggests that the hydrodynamic volume of NAPols in organic solvents is sensitive to solvent polarity. Deprotected NAPols were found to be highly water-soluble and surface-active. DLS, ASEC, and AUC measurements show that they form, in aqueous solution, well-defined supramolecular self-assemblies  $\sim 6$ – $7$  nm in diameter, with a narrow size distribution and an average molecular weight of  $\sim 50 \times 10^3$  g·mol<sup>-1</sup>. This implies that  $\sim 2$  polymeric chains assemble into a particle containing  $\sim 22$ – $28$  hydrophobic chains. This rather low value, when compared, e.g., to that in *n*-undecylmaltopyranoside micelles (number of aggregation  $\sim 71$ ),<sup>61</sup> is likely related to the steric constraints exerted by the bulky hydrophilic moieties. Small differences in the average molar mass and degree of polymerization have little effect on the physicochemical characteristics of the final NAPols, such as particle size and solubility. This is of great interest, from a practical point of view, since it implies that small batch-to-batch variations should not affect their ability to trap IMPs, an application for which they appear well suited.

**Acknowledgment.** Thanks are due to Y. Gohon (UMR 7099; current address: INRA, Thiverval-Grignon, France) for his participation in early biochemistry experiments, to F. Rouvière (UMR 7099) for synthesizing the batch of A8-35 used in the present work, to C. Mathe (LCBOSMV) for access to the FTIR spectrometer, and to S. Périmo and M. Ablá (LCBOSMV) for initial help with syntheses. The authors acknowledge the financial support of the Université d'Avignon et des Pays du Vaucluse, the CNRS, the Université Paris-7, the CEA, and the E.C. Specific Targeted Research Project 5137770 *Innovative tools for membrane structural proteomics (IMPS)*. K.S.S. and T.D. were funded by IMPS. B.O. and T.D. were recipients of fellowships from the

(59) Qiu, Y.; Zhang, T.; Ruegsegger, M.; Marchant, R. E. *Macromolecules* **1998**, *31*, 165–171.

(60) Wang, S.; Marchant, R. E. *Macromolecules* **2004**, *37*, 3353–3359.

(61) Anatrace Catalog, 2008 (<http://www.anatrace.com>).

Ministère de l'Enseignement Supérieur et de la Recherche. P.B. is the recipient of a Marie Curie Early Stage Training fellowship awarded by the BioMem E.C. network.

**Supporting Information Available:** Material, general procedures, and instrumentation for the synthesis; synthesis of compounds **1** and **2**;  $^1\text{H}$ ,  $^{13}\text{C}$  NMR spectra, mass spectra and UV calibration curve of the TA; GPC analysis of different cotelomers; water solubility of

NAPols;  $D_{\text{H}}$  distribution statistical plot for different NAPols obtained by DLS; ASEC chromatograms of dialysable impurities collected after NA20-79 purification; molecular weight estimates obtained by GPC using different solvent systems; particle size in aqueous solution of NA20-78 and NA22-75 at different concentrations and temperatures. This material is available free of charge via the Internet at <http://pubs.acs.org>.

LA8023056

## Supporting Information For

# Glucose-Based Amphiphilic Telomers Designed to Keep Membrane Proteins Soluble in Aqueous Solutions: Synthesis and Physical-Chemical Characterization

*K. Shivaji Sharma<sup>†</sup>, Grégory Durand<sup>†\*</sup>, Fabrice Giusti<sup>‡</sup>, Blandine Olivier<sup>†</sup>, Anne-Sylvie Fabiano<sup>†</sup>, Paola Bazzacco<sup>‡</sup>, Tassadite Dahmane<sup>‡</sup>, Christine Ebel<sup>#</sup>, Jean-Luc Popot<sup>‡</sup> and Bernard Pucci<sup>†\*</sup>*

<sup>†</sup>Laboratoire de Chimie Bioorganique et des Systèmes Moléculaires Vectoriels, Université d'Avignon et des Pays de Vaucluse, Faculté des Sciences, 33 rue Louis Pasteur, F-84000 Avignon, France

<sup>‡</sup>Laboratoire de Physico-Chimie Moléculaire des Membranes Biologiques, UMR 7099, C.N.R.S. and Université Paris-7, Institut de Biologie Physico-Chimique, 13, rue Pierre-et-Marie-Curie, F-75005 Paris, France

<sup>#</sup> CNRS, Institut de Biologie Structurale, Laboratoire de Biophysique Moléculaire, 41 rue Jules Horowitz, Grenoble, F-38027, France. CEA, DSV, IBS, Grenoble, F-38027, France. Université Joseph Fourier, Grenoble, F-38000, France.

gregory.durand@univ-avignon.fr

bernard.pucci@univ-avignon.fr

Table of contents		Pages
Materials, general procedure and instrumentation for the synthesis.		S2
Synthesis of compound <b>1</b> and <b>2</b> .		S3
Determination of Monomers ratio (x/y) by <sup>1</sup> H NMR.		S4
Determination of number average degree of polymerization ( <i>DP<sub>n</sub></i> ).		S4
<b>Figure S1</b>	<sup>1</sup> H and <sup>13</sup> C NMR spectrum of telogen agent ( <b>2</b> ) in CDCl <sub>3</sub> .	S5
<b>Figure S2</b>	Mass spectra of telogen agent ( <b>2</b> ).	S6
<b>Figure S3</b>	UV calibration curve of telogen agent ( <b>2</b> ).	S7
<b>Figure S4</b>	GPC traces of different cotelomers in THF + 0.1% TFA and DMF.	S7
<b>Figure S5</b>	Measurement of water solubility of NA25-78 at rt.	S8
<b>Figure S6</b>	Evolution as a function of concentration of the hydrodynamic diameter of the particles formed by different NAPols in water at 25°C.	S8
<b>Figure S7</b>	Hydrodynamic diameter distribution statistical plot (by volume) from DLS.	S9
<b>Figure S8</b>	SEC chromatograms of NA22-75 before and after dialysis (Superose 12 10-300GL column, detection at 220 nm; V <sub>e</sub> = 13.0 mL).	S10
<b>Figure S9</b>	SEC chromatograms of impurities separated from NA20-79 during dialysis (Superose 12 10-300GL column, detection at 220 nm).	S10
<b>Table S1</b>	GPC results of protected cotelomers using different solvents system.	S11
<b>Table S2</b>	Particle size distribution by volume (from DSL) of NA20-78 in aqueous solution at different temperatures.	S12
<b>Table S3</b>	Particle size distribution by volume (from DSL) of NA20-78 and NA22-75 in aqueous solution at various concentrations at 25°C.	S12

**Materials.** Starting materials were obtained either from Acros Organics or Aldrich and used as received unless otherwise stated. The initiator (AIBN) was used after recrystallization in ethanol. Thin-layer chromatography (TLC) was performed on silica gel plates (Merck Kieselgel 60F<sub>254</sub>), and preparative column chromatography was employed on Merck Si-60 silica gel (40-63  $\mu\text{m}$ ). For polymerization reactions, the THF was dried over sodium-benzophenone ketyl and refluxed and distilled under argon prior to use. Ion exchange resin Amberlite IRC-50 was from Sigma. Size exclusion chromatography was carried out on Sephadex<sup>TM</sup> LH-20 resin (GE Healthcare Bio-sciences, Sweden). For GPC measurements, THF (stabilized with 0.025 % BHT) and DMF of Analytical range grade (>99%), LiBr, LiNO<sub>3</sub>, tetra *n*-butylammonium bromide (>99%), and Trifluoroacetic acid (TFA, Fluorochem Ltd., UK) were used as received. Water was deionized with a Millipore Milli-Q system. Cellulose dialysis membrane ( $M_w$  cut-off 6-8 x 10<sup>3</sup> g.mol<sup>-1</sup>) was from Spectra/Por.

**General procedure and instrumentation for the synthesis.** Progress of the reactions and homogeneity of the compounds were monitored by TLC. Compounds were detected by exposure to ultraviolet light ( $\lambda = 254$  nm) and by spraying of sulphuric acid (5% ethanol) and/or ninhydrin (5% ethanol) followed by heating at  $\sim 150^\circ\text{C}$  to detect glucose- and amine- containing groups, respectively. The <sup>1</sup>H, <sup>13</sup>C and DEPT NMR sequences were recorded on a Bruker AC-250 spectrometer. Chemical shifts are given in ppm relative to the solvent residual peak as a heteronuclear reference. Abbreviations used for signal patterns are: s (singlet), d (doublet), t (triplet), q (quartet), m (multiplet). UV-Vis-spectra were recorded on a Cary Win Varian Spectrophotometer with a double-compartment quartz cell of 10-mm length (Suprasil). FT-IR spectra were recorded on a Nicolet (Madison, Wisconsin, USA) Avatar 360 ESP spectrometer equipped with a DTGS KBr detector and controlled by EZ OMNIC 6.0 software. Numerical data were obtained after 64 scans with 4-cm<sup>-1</sup> sensitivity. Mass spectrometry was recorded on a Triple quadrupole spectrometer API III Plus Sciex for ESI+. Melting points were measured on an Electrothermal IA9100 apparatus. All the solvents were of reagent grade and distilled and dried according to standard procedures prior to use.

***N*-((Trishydroxymethyl)-methyl)-3-tritylsulfanyl-propionamide (1).** A solution of 3-mercaptopropanoic acid (6 g, 56.5 mmol, 1 equiv.) in CH<sub>2</sub>Cl<sub>2</sub> (30 mL) was added dropwise to a solution of triphenylmethyl chloride (17.3 g, 62.2 mmol, 1.1 equiv.) in CH<sub>2</sub>Cl<sub>2</sub>. The mixture was stirred 16 h at room temperature, then filtered and concentrated under vacuum to give 3-tritylsulfanyl-propionic acid (18.7 g, 53.7 mmol, 95%) as a white powder. 3-tritylsulfanyl-propionic acid (8.5 g, 24.3 mmol, 1 equiv.), tris(hydroxymethyl)aminomethane (3.3 g, 26.7 mmol, 1.1 equiv.) and EEDQ (7.2 g, 29.1 mmol, 1.2 equiv.) were dissolved in ethanol (30 mL). The mixture was stirred at 50°C for 12 h, then filtered and concentrated under vacuum. The crude mixture was recrystallized from ether to give compound **1** (8.6 g, 19.0 mmol, 79%) as a white powder. *R<sub>f</sub>*~0.4, ethylacetate. Mp 140-145°C. <sup>1</sup>H NMR (250 MHz, CDCl<sub>3</sub>) δ 7.55-7.15 (m, 15H), 6.37 (s, 1H), 5.17 (s, 3H), 3.53 (s, 6H), 2.54 (t, *J* = 6.9 Hz, 2H), 1.97 (t, *J* = 6.9 Hz, 2H). <sup>13</sup>C NMR (62.86 MHz, CDCl<sub>3</sub>) δ 173.1 (CO), 144.6 (C), 129.5, 128.0, 126.8 (CH), 66.9 (C), 62.1 (CH<sub>2</sub>), 61.2 (C), 35.8, 27.8 (CH<sub>2</sub>).

***N*-((Tris benzyloxymethyl)-methyl)-3-mercapto-propionamide (2).** Compound **1** (5.0 g, 11.1 mmol, 1 equiv.) and triethylamine (14.0 mL, 99.6 mmol, 9 equiv.) were dissolved in CH<sub>2</sub>Cl<sub>2</sub>. A solution of benzoyl chloride (5.8 mL, 49.8 mmol, 4.5 equiv.) in CH<sub>2</sub>Cl<sub>2</sub> was added dropwise. The mixture was stirred for 12 h at room temperature, then poured into cold water. The organic layer was dried over Na<sub>2</sub>SO<sub>4</sub>, filtered and concentrated under vacuum to give *N*-((Trisbenzyloxymethyl)methyl)-3-tritylsulfanyl-propionamide (7.6 g, 10.2 mmol, 92%) as a white powder. This compound (6.0 g, 8.0 mmol) was dissolved in a TFA/CH<sub>2</sub>Cl<sub>2</sub> (2:8 v/v) mixture at 0°C. After addition of few drops of triethylsilane the mixture was stirred for 4 h at ambient temperature, then concentrated under vacuum. The crude mixture was purified by flash chromatography, eluting with ethylacetate/cyclohexane (3:7 v/v), followed by recrystallization from CH<sub>2</sub>Cl<sub>2</sub>/*n*-hexane to give compound **2** (2.5 g, 4.8 mmol, 60%) as a white powder. *R<sub>f</sub>*~0.8, ethylacetate/cyclohexane (7:3 v/v). Mp 137-141°C. <sup>1</sup>H NMR (250 MHz, CDCl<sub>3</sub>) δ 8.2-7.4 (m, 15H), 6.59 (s, 1H), 4.94 (s, 6H), 2.80 (q, *J* = 7.1 Hz, 2H), 2.56 (t, *J* = 6.6 Hz, 2H), 1.60 (t, *J* = 8.4 Hz, 1H). <sup>13</sup>C NMR (62.86 MHz, CDCl<sub>3</sub>) δ 171.3, 166.4 (CO), 133.5 (C), 129.8, 129.2, 128.6 (CH), 63.7 (CH<sub>2</sub>), 59.3 (C), 41.0, 20.3 (CH<sub>2</sub>). MS (ESI+, *m/z*) 522.2 [M + H]<sup>+</sup>; 539.3 [M + NH<sub>4</sub>]<sup>+</sup>; 544.2 [M + Na]<sup>+</sup>.

### Determination of Monomers ratio (x/y) by <sup>1</sup>H NMR.

The monomer ratio (x/y) in the protected cotelomer was estimated by comparing the peak integrals assigned to three specific protons of the glucose moieties (H<sub>4</sub>, H<sub>3</sub> and H<sub>2</sub>) from both the monomers **A** and **B** (or **B'**) with the NH-vicinal methylene group of the alkyl chain from only monomer **B** (or **B'**) in <sup>1</sup>H NMR spectra (Figure 2 B in main article). Let “x” be the fraction number of monomer **A**, “y” the fraction number of monomer **B** (or **B'**), and H<sub>Glu</sub> and H<sub>Chain</sub> the area for the respective peaks observed, we can write the two equations,

$$3(x + y) = \alpha H_{\text{Glu}} \quad (1)$$

$$2y = \alpha H_{\text{Chain}} \quad (2)$$

$\alpha$  is a constant. By assigning 2 for H<sub>chain</sub> during the NMR integration, *i.e.*  $y/\alpha = 1$ , then we get easily the value for x/y and evaluate the relative values of x and y (whole numbers).

### Number average degree of polymerization (DP<sub>n</sub>) of Cotelomer.

The DP<sub>n</sub> of the telomers were determined by combining <sup>1</sup>H NMR and UV data through the following equations

$$M_{\text{cotelomer}} = M_{\text{TA}} + [(x M_{\text{MA}}) + (y M_{\text{MB}})] * n \quad (4)$$

$$M_{\text{cotelomer}} = 522 + [x*589 + y*702]*n \quad \text{for monomer A and B} \quad (5)$$

$$M_{\text{cotelomer}} = 522 + [x*589 + y*744]*n \quad \text{for monomer A and B'} \quad (6)$$

$M_{\text{TA}}$  is the molecular mass of the telogen agent,  $M_{\text{MA}}$  and  $M_{\text{MB}}$  those of monomers **A** and **B** (or **B'**), respectively,  $n$  the total number of monomers **A** and **B** (or **B'**). The number average degree of polymerization DP<sub>n</sub> is then easily obtained:

$$DP_n = n(x+y) + 1 \quad (7)$$

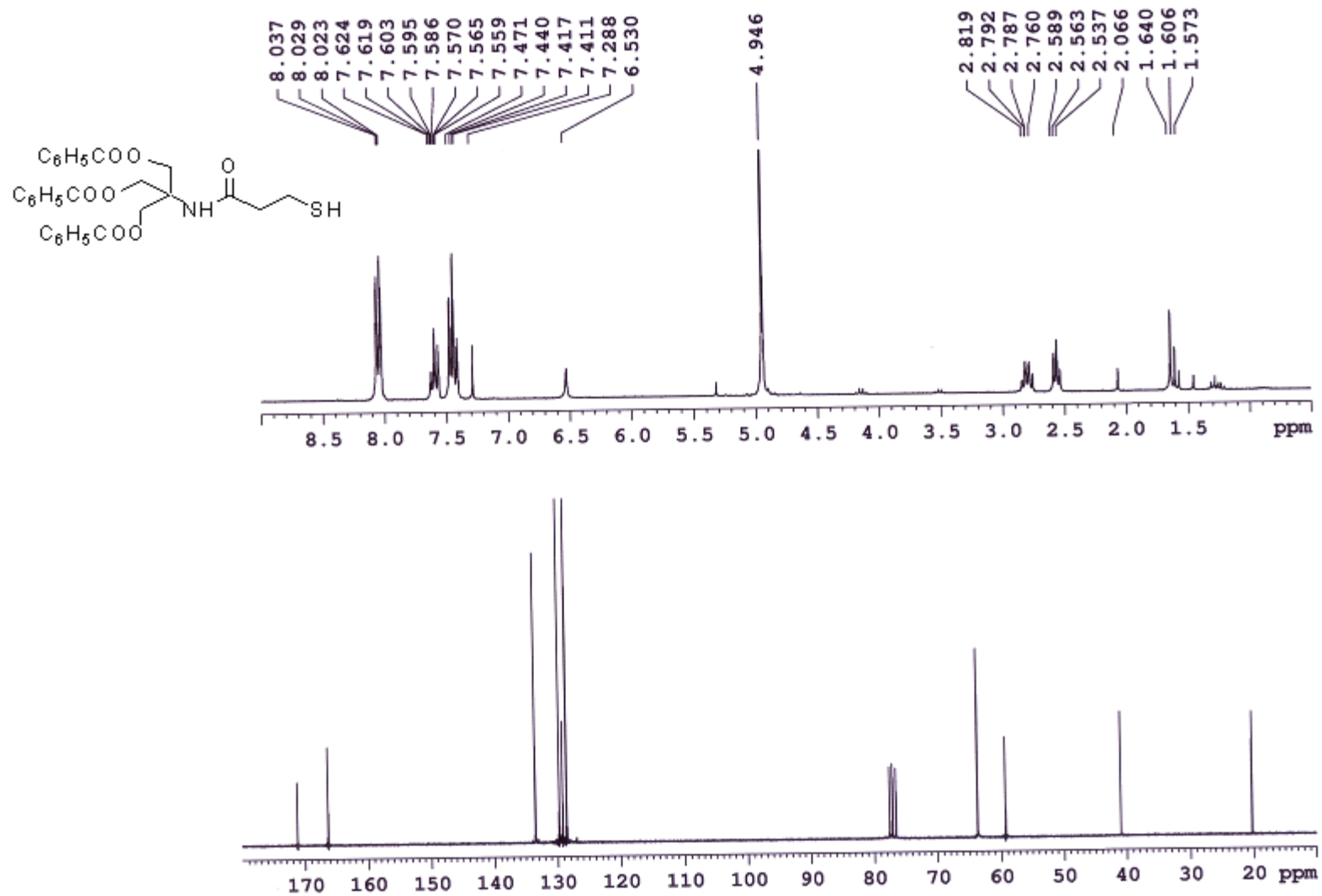


**Figure S1.** <sup>1</sup>H and <sup>13</sup>C NMR spectrum of telogen agent (2) in CDCl<sub>3</sub>.

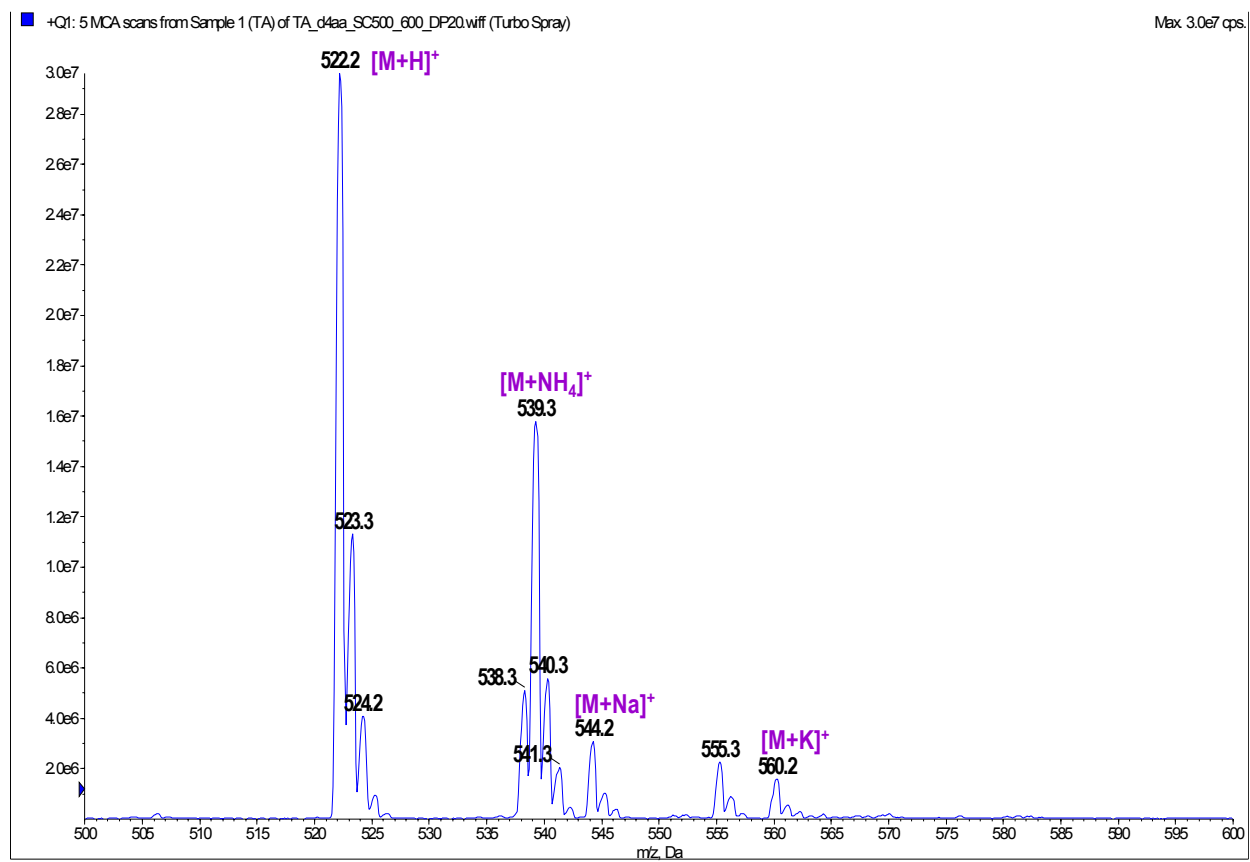
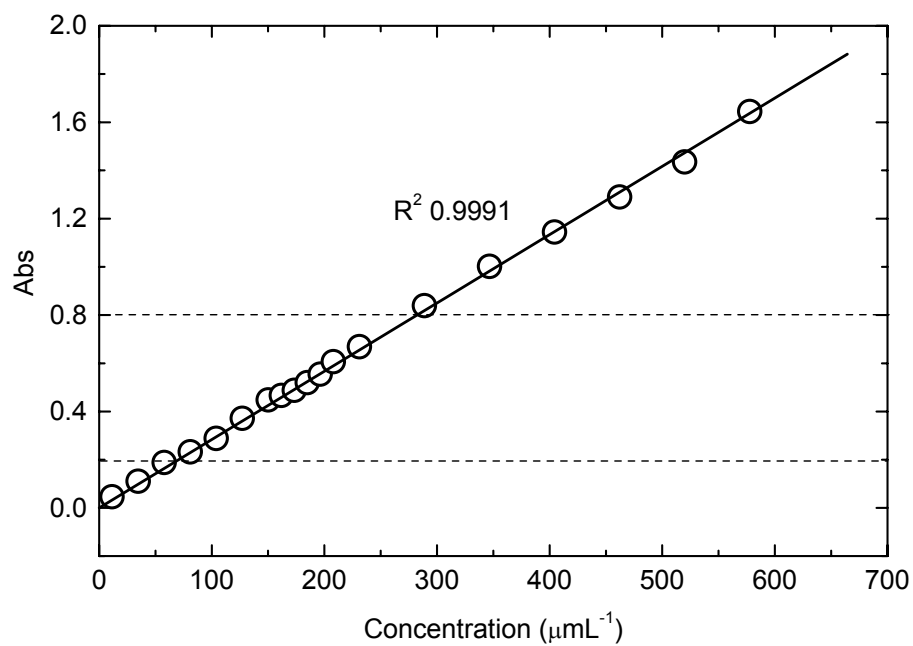
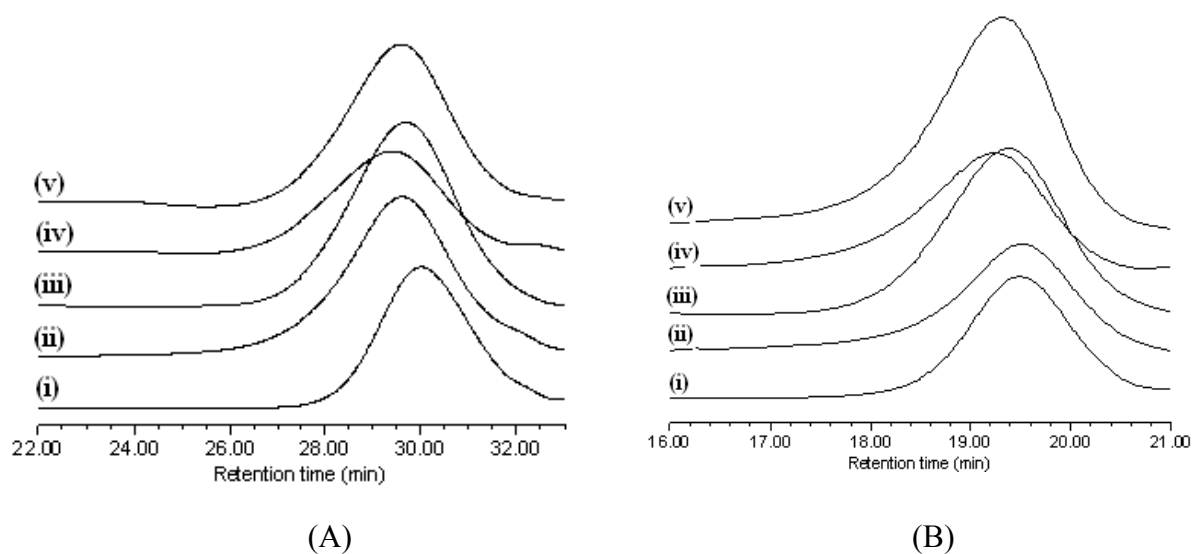


Figure S2. Mass Spectra of telogen agent (2).



**Figure S3.** UV calibration curve of telogen agent (**2**) (at  $\lambda_{\max} = 272$  nm, 25°C).



**Figure S4.** GPC traces of different cotelomers using (A) THF + 0.1% TFA, (B) DMF: (i) NA22-83, (ii) NA22-75, (iii) NA20-78, (iv) NA29-83, (v) NA25-78.

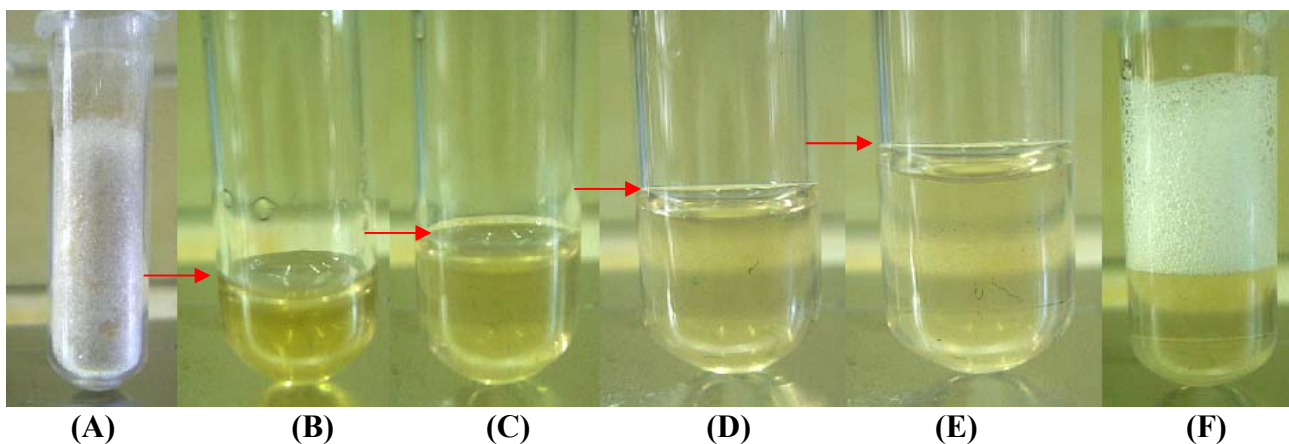


**Figure S5.** Measurement of water solubility of NA25-78 at rt. (A) 100 mg of lyophilised and dried sample. (B) Same in 250  $\mu\text{L}$  of water ( $400\text{g.L}^{-1}$ ), (C) in 500  $\mu\text{L}$  of water ( $200\text{g.L}^{-1}$ ), (D) in 750  $\mu\text{L}$  of water ( $133.3\text{ g.L}^{-1}$ ), (E) in 1 ml of water ( $100\text{ g.L}^{-1}$ ); solutions C-E are limpid, indicating a solubility above  $200\text{ g.L}^{-1}$ . (F) Shaking by hand the mixture gave foam, which was stable for at least 2 h at rt.

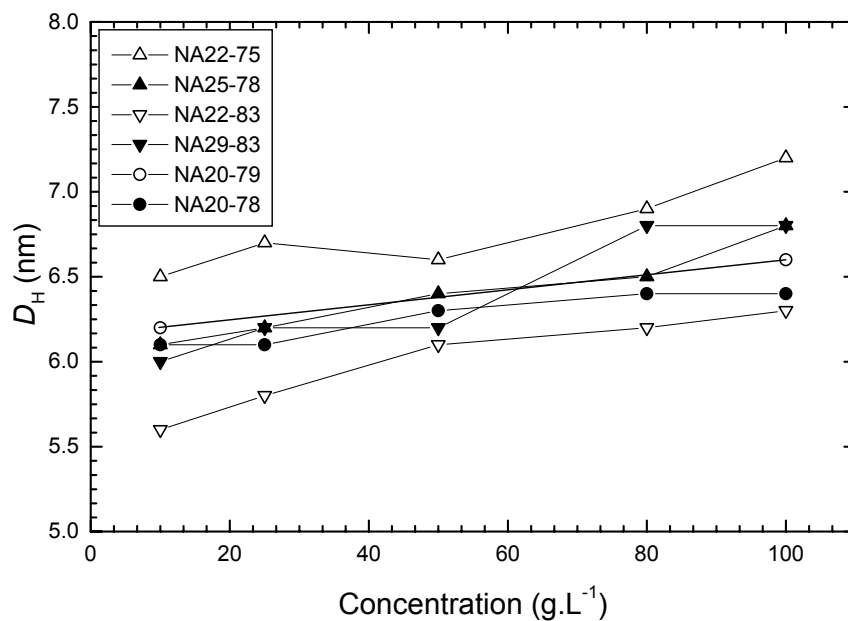


**Figure S6.** Evolution as a function of concentration of the hydrodynamic diameter of the particles formed by different NAPols at  $25^{\circ}\text{C}$  in water, as measured by DLS.

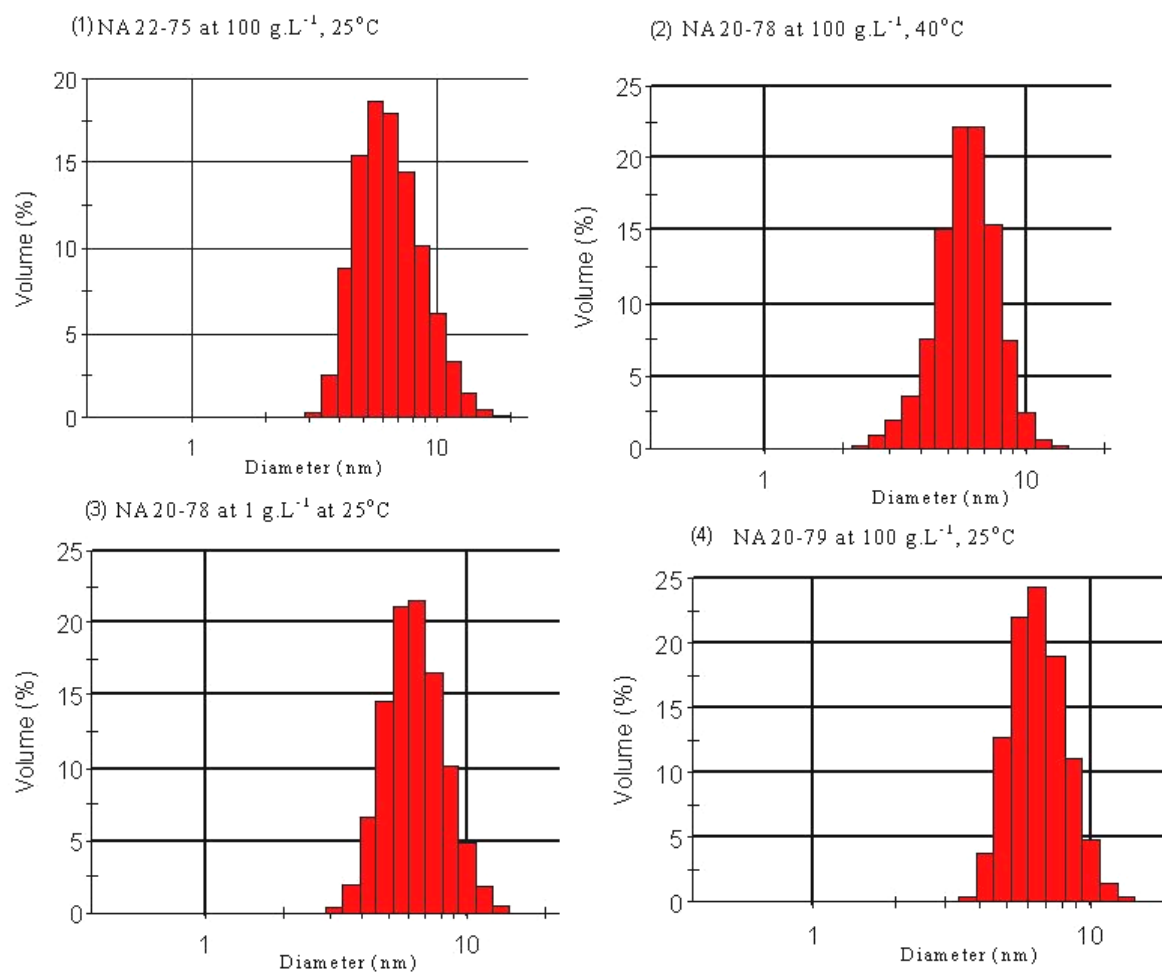


**Figure S7.** Hydrodynamic diameter distribution statistical plot (by volume) of different NAPols from DLS.

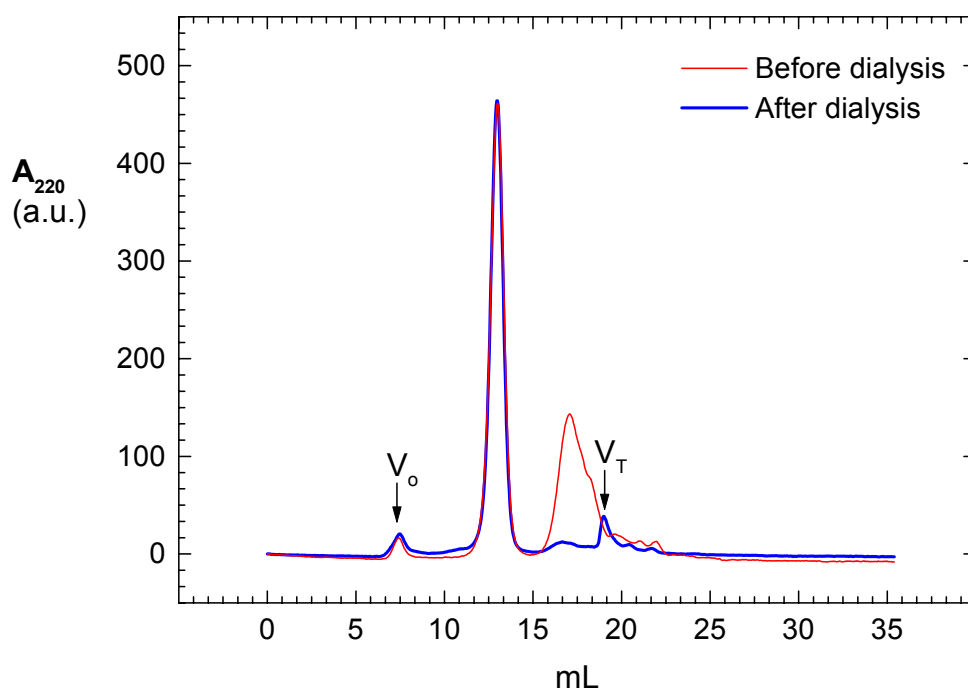


**Figure S8.** SEC chromatograms of NA22-75 before and after dialysis (Superose 12 10-300GL column, elution with Tris buffer ([Tris-HCl/Tris] = 20 mM, [NaCl] = 100 mM, pH = 8.5), detection at 220 nm; in both samples, the main particles elute at  $V_e = 13.0$  mL).

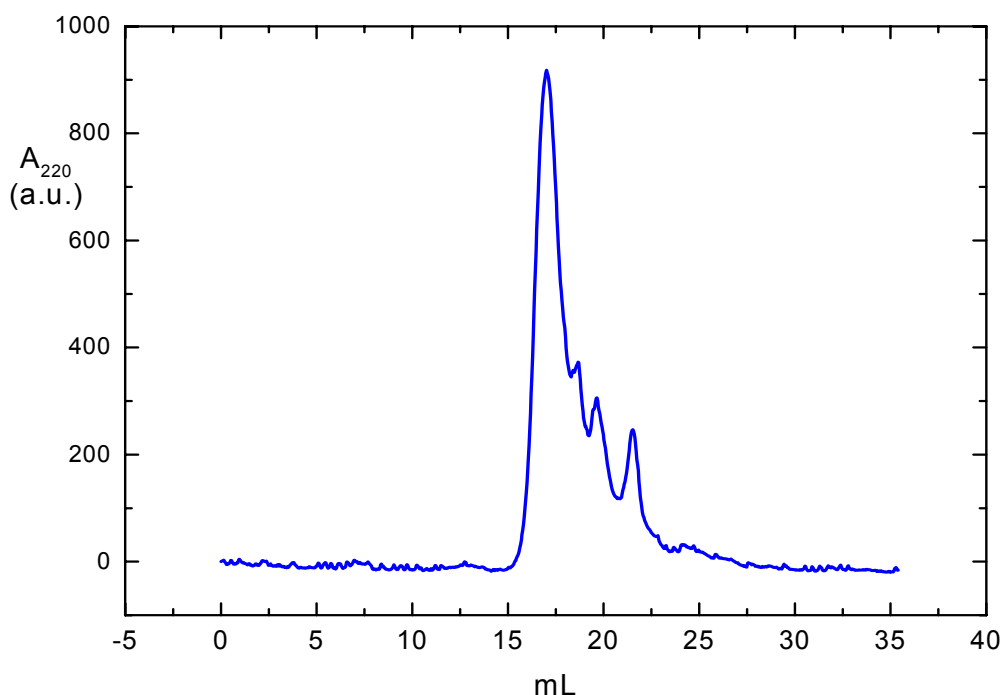


**Figure S9.** SEC chromatograms of impurities separated from NA20-79 during dialysis (Superose 12 10-300GL column, elution with Tris buffer ([Tris-HCl/Tris] = 20 mM, [NaCl] = 100 mM, pH = 8.5), detection at 220 nm). 16 mg of the exterior dialyzed materials were put in suspension in 500  $\mu$ L of mQ water. The suspension was stirred for 1 day and centrifuged. The supernatant was taken off and injected on a Superose 10-300GL column.

**Table S1.** GPC results of protected cotelomers using different solvents system.

NAPol	THF			THF + 0.1% TFA			DMF			DMF + 0.01M LiBr		
	$\bar{M}_w^a/10^3$	$\bar{M}_n^b/10^3$	PDI <sup>c</sup>	$\bar{M}_w/10^3$	$\bar{M}_n/10^3$	PDI	$\bar{M}_w/10^3$	$\bar{M}_n/10^3$	PDI	$\bar{M}_w/10^3$	$\bar{M}_n/10^3$	PDI
NA22-75	4.77	3.80	1.26	6.33	5.66	1.12	10.69	10.08	1.06	12.65	11.92	1.06
NA25-78	4.87	3.61	1.35	5.96	5.53	1.08	12.56	10.90	1.15	13.52	12.65	1.07
NA22-83	3.45	3.06	1.13	5.07	4.83	1.05	9.66	9.43	1.02	11.95	11.47	1.04
NA29-83	7.14	4.45	1.61	6.36	5.84	1.09	11.49	10.72	1.07	14.37	13.45	1.07
NA20-78 <sup>d</sup>	5.00	3.96	1.26	5.86	5.45	1.08	10.50	10.09	1.04	13.37	12.65	1.06

<sup>a</sup>Weight-average molecular weight ( $\text{g}\cdot\text{mol}^{-1}$ ). <sup>b</sup>Number-average molecular weight ( $\text{g}\cdot\text{mol}^{-1}$ ). <sup>c</sup>Polydispersity Index ( $\bar{M}_w/\bar{M}_n$ ) were evaluate by GPC using PMMA standard. <sup>d</sup>Synthesized with monomer **B**'.

**Table S2.** Particle size distribution by volume (from DSL) of NA20-78 in aqueous solution at different temperatures.

Concentration (g.L <sup>-1</sup> )	Temperature (°C)				
	10	25	40	60	80
100	6.7 <sup>a</sup> (2.0) <sup>b</sup>	6.4 (2.0)	6.4 (1.9)	6.2 (1.8)	6.4 (1.8)
1.0	6.0 (1.5)	6.2 (1.4)	6.0 (1.5)	5.8 (1.5)	6.1 (1.6)

<sup>a</sup>  $D_H$ , hydrodynamic diameter (nm). <sup>b</sup> HHW (nm), the width of the peak at half-height, an indication of the degree of polydispersity of the aggregates.

**Table S3.** Particle size distribution by volume (from DSL) of NA20-78 and NA22-75 in aqueous solution at various concentrations at 25°C.

NAPol	Concentration (g.L <sup>-1</sup> )								
	1	0.1	0.09	0.08	0.07	0.06	0.05	0.01	0.005
NA20-78	5.9 <sup>a</sup> (1.5) <sup>b</sup>	6.3 (1.4)	5.7 (1.8)	7.6 (3.8)	9.4 (3.0)	7.6 (3.5)	7.3 (3.2)	6.6 (1.8)	- <sup>c</sup>
NA22-75	6.1 (1.5)	6.7 (2.7)	7.3 (2.8)	6.8 (2.3)	7.8 (3.9)	7.6 (1.9)	- <sup>c</sup>	- <sup>c</sup>	- <sup>c</sup>

<sup>a</sup>  $D_H$ , the hydrodynamic diameter (nm). <sup>b</sup> HHW (nm), the width of the peak at half-height, is an indication of the degree of polydispersity of the aggregates. <sup>c</sup>For NA20-78, the particles size could be specified up to a concentration of 0.01 g.L<sup>-1</sup> while for NA22-75 it was 0.06 g.L<sup>-1</sup>.